**Universidade do Minho**
Escola de Medicina

Adriana Faria Gonçalves

# Evaluation of a mutation on 26S proteasome subunit of *Plasmodium falciparum* towards antimalarial resistance

dezembro de 2021

Evaluation of a mutation on 26S proteasome subunit of *Plasmodium falciparum* towards antimalarial resistance

AdrianaGonçalves

UMinho | 2021

**Universidade do Minho**
Escola de Medicina

Adriana Faria Gonçalves

# Evaluation of a mutation on 26S proteasome subunit of *Plasmodium falciparum* towards antimalarial resistance

Dissertação de Mestrado
Mestrado em Ciências da Saúde

Trabalho efetuado sob a orientação do
**Professor Doutor Pedro Eduardo Mendes Ferreira**

dezembro de 2021

## DIREITOS DE AUTOR E CONDIÇÕES DE UTILIZAÇÃO DO TRABALHO POR TERCEIROS

# Acknowledgments

With the culmination of one of the most challenging years of my life, which was without a doubt an enormous growth, both scientifically and personally, I can only express my sincere thanks to everyone who made its conclusion possible.

Firstly, I want to thank my supervisor, Doctor Pedro Ferreira, for his support, motivation, and constant knowledge sharing. Thank you for all your help and patience throughout this dissertation.

To my group members, a special acknowledgment for all your availability to clarify doubts, for all the help given, and for all the patience. To Rita, I would like to thank you for making me part of the team and the laboratory. You were my biggest support throughout this year and this master. Thank you so much for your friendship.

I also want to thank all the colleagues in the lab for all the companionship, constant help, and all advice. A special thanks to Ana Frias, Ana Mendes, Consuelo, and Maria João for integrating and supporting me.

To all my friends, cenas, esquadrão, Rui, Adriana and tias, especially Sara. Your friendship and your joy were essential to overcome the daily frustrations. I want to thank you for all the fellowship and the silly discussions that brightened my day, for always being there to talk and judge, and for all the fun moments. Thank you for always supporting me in my bad moods and existential crisis.

Finally, I want to thank my parents, my sister, and Tiago, without them, this journey would not have been possible. I also want to thank my entire family for all the love, encouragement, and pride they show in me and for always being there. Thank you for believing in me.

The work presented in this thesis was performed in the Life and Health Sciences Research Institute (ICVS), University of Minho. Financial support was provided by grants from the National funds, through the Foundation for Science and Technology (FCT) - project UIDB/50026/2020, UIDP/50026/2020, IF/00143/2015/CP1294/CT0001 and PTDC/SAU-PAR/28066/2017.

## STATEMENT OF INTEGRITY

I hereby declare having conducted this academic work with integrity. I confirm that I have not used plagiarism or any form of undue use of information or falsification of results along the process leading to its elaboration.

I further declare that I have fully acknowledged the Code of Ethical Conduct of the University of Minho.

# Resumo

**Avaliação de uma mutação numa subunidade do proteossoma 26S do *Plasmodium falciparum* em relação à resistência aos antimaláricos**

Malária continua a ser uma das principais causas de morte em todo o mundo, especialmente nas regiões tropicais. Esta é causada por parasitas protozoários do género *Plasmodium*, sendo o *P. falciparum* a espécie mais virulenta em humanos, devido à sua capacidade de citoaderência, obstruindo a perfusão e, consequentemente, evitando a depuração pelo sistema imunitário. Ao longo dos anos, várias terapias já foram utilizadas sendo as terapias combinadas com base na artemisinina (ACTs) as mais utilizadas atualmente. A artemisinina ativada presumivelmente gera dano celular ao reagir com os grupos suscetíveis das biomoléculas. Estas são posteriormente marcadas com ubiquitina de modo a serem reconhecidas e degradadas pelo proteossoma. No entanto, resistência à artemisinina já foi relatada e é necessário compreender os mecanismos envolvidos para não permitir que se espalhe enquanto ainda está muito localizada em regiões específicas do globo.

Num laboratório parceiro, uma variante de um nucleótido foi encontrada no gene *rpn2*, causando a variação não-sinónima E738K, em parasitas da espécie *P. chabaudi* resistente a ACTs. Este projeto tem o objetivo de avaliar o impacto da variante, localizada no gene *rpn2*, uma subunidade da partícula regulatória 19S do proteossoma, na função fisiológica do parasita e na resposta à artemisinina. Para isso, dois plasmídeos foram construídos contendo as duas variantes E738 e 738K, usando partes do gene *rpn2* do *P. falciparum* e a parte do *P. chabaudi* onde a variante está localizada. Estes genes quiméricos foram criados devido a uma homologia de 78.6% entre as proteínas das duas espécies e também devido à dificuldade associada ao manuseamento *in vitro* dos parasitas da espécie *P. chabaudi*.

Nos ensaios de suscetibilidade na resposta à dihidroartemisinina (DHA), os parasitas $26S^{738K}$ apresentaram maior resistência e sobrevivência em estágio de anel, comparativamente aos parasitas $26S^{E738}$. Relativamente ao impacto fisiológico, estes também apresentaram uma estabilização na atividade do proteossoma quando expostos a DHA, resultando numa redução da acumulação de proteínas poliubiquitinadas. Pelo contrário, em parasitas com a variante E738, uma diminuição da atividade do proteossoma e um aumento das proteínas após reação com DHA foi observado. Estes resultados sugerem que a variante 738K detetada em *P. chabaudi* confere resistência à DHA em *P. falciparum* e que o proteossoma está diretamente envolvido no mecanismo de resistência. Para além disso, demonstra que a via ubiquitina-proteossoma desempenha um papel importante no mecanismo de ação da DHA.



**Palavras-chave:** *Plasmodium falciparum*; proteossoma 26S; resistência à artemisinina.

# Abstract

**Evaluation of a mutation on 26S proteasome subunit of *Plasmodium falciparum* towards antimalarial resistance**

Malaria remains one of the leading causes of mortality worldwide, especially in tropical regions. This disease is caused by a protozoan parasite of the *Plasmodium* genus, with *P. falciparum* being the most virulent species capable of infecting humans due to its ability of cytoadherence, obstructing perfusion and, consequently, evading immune system clearance. Multiple therapies have been used over the years, with artemisinin-based combination therapies (ACTs) being the most widely used today. Activated artemisinin presumably generates cellular damage by reacting with the susceptible groups of biomolecules. These are posteriorly marked with ubiquitin to be recognized and degraded by the 26S proteasome. However, artemisinin resistance has emerged, and it is necessary to understand its mechanisms not to allow its spread while it is very located.

A partner group laboratory found a single nucleotide variant (SNV), causing a non-synonymous mutation, the E738K, in the *rpn2* gene, on ACT resistant *P. chabaudi* parasites. Therefore, this project aimed to evaluate the impact of the E378K variant, located in the *rpn2* gene, a subunit of the 19S regulatory particle of the 26S proteasome, on the proteasome function in the parasite life cycle and in the artemisinin response. Two plasmids were constructed bearing the E738 and 738K variants, using parts of the *P. falciparum rpn2* gene and the part of the *P. chabaudi rpn2* gene where the variant is located. These chimeric genes were created due to a 78.6% homology between the proteins of both species and the impossibility to culture *P. chabaudi* parasite *in vitro*.

Drug susceptibility assays showed that the $26S^{738K}$ parasites presented a higher $IC_{50}$ and higher parasite survival in the ring-stage survival assay (RSA), compared to the $26S^{E738}$ parasites, in the artemisinin response. Additionally, they presented a stabilization in the proteasome activity when challenged to dihydroartemisinin (DHA) and consequent reduction of polyubiquitinated proteins accumulation. On the contrary, E738 parasites showed a decrease in the proteasome activity and increased polyubiquitinated proteins upon reaction with DHA. These results suggest that the 738K variant confer DHA resistance to the parasites and that the proteasome is involved in this DHA resistance. Moreover, it demonstrates that the ubiquitin-proteasome pathway plays an important role in the DHA mechanism of action.



**Keywords:** 26S Proteasome*;* Artemisinin resistance; *Plasmodium falciparum*.

# Table of Contents

# Figure Index

# Table Index

# List of Abbreviations and Acronyms

| | |
|---|---|
| **ACTs** | Artemisinin-Based Combination Therapies |
| **AMC** | 4-amino-7-methylcoumarin |
| **APPs** | Aminopepetidases |
| **ART** | Artemisinin |
| **ARTs** | Artemisinin and its derivatives |
| **bp** | Base pairs |
| **BTB/POZ** | Broad complex_Tramtrack_bric-a-brac/Pox virus_Zinc finger |
| **BSA** | Bovine Serum Albumin |
| **CP** | Core Particle |
| **DHA** | Dihydroartemisinin |
| **DMSO** | Dimethyl Sulfoxide |
| **DUBs** | Deubiquitinases |
| **E** | Glutamic Acid |
| **eIF2α** | Eukaryotic Factor-2α |
| **E1** | Ubiquitin-activating Enzyme |
| **E2** | Ubiquitin-conjugating Enzyme |
| **E3** | Ubiquitin Ligase |
| **E4** | Chain-elongation Enzyme |
| **ER** | Endoplasmic Reticulum |
| **gDNA** | Genomic DNA |
| **GHTM/IHMT** | Global Health & Tropical Medicine/Instituto de Higiene e Medicina Tropical |
| **GMS** | Greater Mekong Subregion |
| **GTS** | WHO Global Technical Strategy for Malaria 2016-2030 |
| **hDHFR** | human Dihydrofolate Reductase |
| **HF** | High-Fidelity |
| **$IC_{50}$** | Half-Maximum Inhibitory Concentration |
| **iRBCs** | Infected Red Blood Cells |
| **ITNs** | Insecticide-Treated Mosquito Nets |
| **IVCC** | Innovative Vector Control Consortium |
| **K** | Lysine |

| | |
|---|---|
| **LB** | Lysogeny Broth |
| **LLIN** | Long-Lasting Insecticide Nets |
| **MAPK** | Mitogen-Activated Protein Kinase |
| **MCM** | Malaria Culture Medium |
| **MDGs** | Millennium Development Goals |
| **p** | Primers |
| **PBS** | Phosphate Buffered Saline |
| **PCR** | Polymerase Chain Reaction |
| ***Pf*EMP1** | *P. falciparum* Erythrocyte Membrane Protein 1 |
| ***Pf*K13** | *P. falciparum* Kelch 13 |
| ***Pf*PI3K** | *P. falciparum* Phosphatidylinositol-3-kinase |
| **PGDH** | Peptidylglutamyl-peptide Hydrolytic |
| **PI3P** | Phosphatidylinositol-3-phosphate |
| **PK4** | *Plasmodium* eIF2α kinase |
| **PROSC** | *Plasmodium* Reactive Oxidative Stress Complex |
| **pSLI** | Selection-Linked Integration plasmid |
| **RBCs** | Red Blood Cells |
| **RIFIN** | Repetitive Interspersed Repeats |
| **RP** | Regulatory Particle |
| **rpm** | Rotations per minute |
| **rpn** | Regulatory Particle Non-ATPase |
| **rpt** | Regulatory Particle ATPase |
| **RSA** | Ring-Stage Survival Assay |
| **RT** | Room Temperature |
| **SDS-PAGE** | Sodium Dodecyl Sulphate-Polyacrylamide Gel Electrophoresis |
| **SEM** | Standard Error of the Mean |
| **SLI** | Selection-Linked Integration |
| **SNV** | Single-Nucleotide Variant |
| **SOC** | Super Optimal broth with Catabolite repression |
| **STEVOR** | Subtelomeric Variant Open Reading Frame |
| **TBS** | Tris-Buffered Saline |
| **TCP** | Tailless Complex Polypeptide |

| | |
|---|---|
| **TRiC** | TCP-1 Ring Complex |
| **TRAC** | Tracking Resistance to Artemisinin Collaboration |
| **UBA** | Ubiquitin-Associated Domain |
| **UBL** | Ubiquitin-Like Domain |
| **UPP** | Ubiquitin Protein Pathway |
| **UPR** | Unfolded Protein Response |
| **UPS** | Ubiquitin-Proteasome System |
| **USPs** | Ubiquitin-specific Proteases |
| **VSA** | Variant Surface Antigens |
| **WHO** | World Health Organization |
| **WT** | Wild Type |

# 1. Introduction

## 1.1. Malaria Epidemiology

Malaria, a mosquito-borne disease, remains a major public health threat worldwide. It is estimated to have caused 229 million infections and 409 thousand deaths in 2019, of which 67% were children under the age of five. The Africa region is the most affected, accounting for 82% of all cases and 94% of all deaths, followed by the South-East Asia region (World Health Organization, 2020).

Despite these numbers, malaria case incidence reduced from 80 cases per 1000 population at risk in 2000 to 57 in 2019, as well as the mortality rate that was reduced from 25 deaths per 100 000 population at risk in 2000 to 10 in 2019 (World Health Organization, 2020). This reduction was mainly due to increased control and elimination programs using artemisinin-based combination therapies (ACTs) along with the increased access to insecticide-treated mosquito nets, improved healthcare systems, increased urbanization, and reduced poverty (Weiss et al., 2019). As a result, it is estimated that a total of 1.5 billion malaria cases and 7.6 million deaths have been averted since 2000 (World Health Organization, 2020).

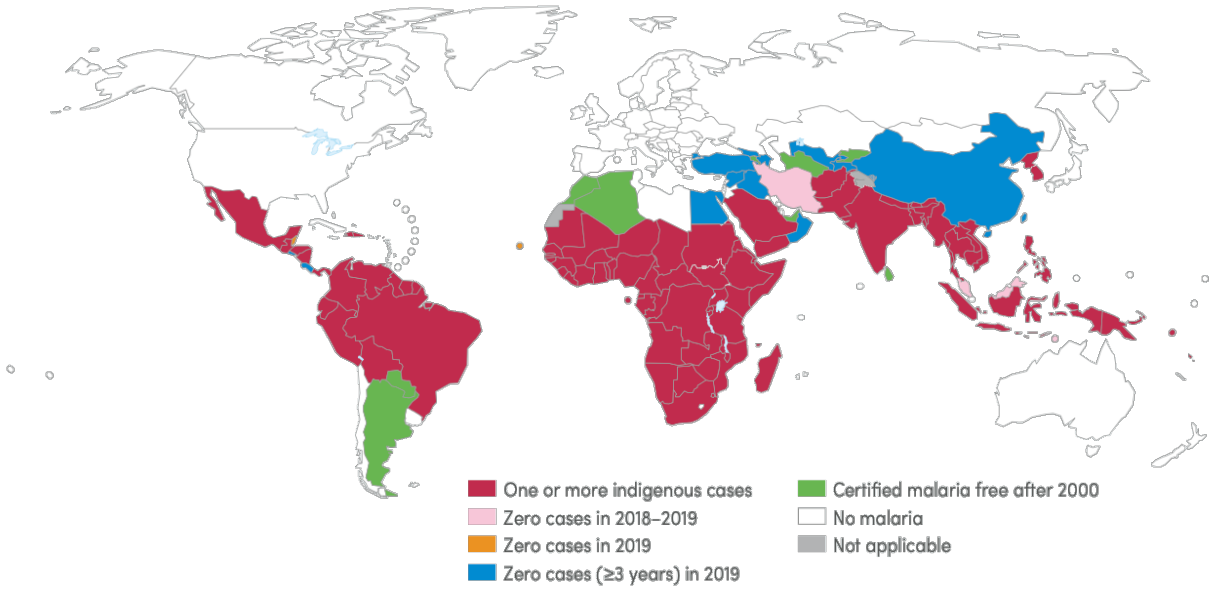


**Figure 1. Countries with indigenous cases in 2000 and their status in 2019.** Countries with zero indigenous cases over at least the past three years are considered to have eliminated malaria, as it is the case of China and El Salvador, which have reported, in 2019, zero indigenous cases for the third consecutive year (World Health Organization, 2020).

## 1.2. Malaria control and elimination

Since the end of the Global Malaria Eradication Programme, in 1969, up to the year 2000, little was done to eradicate malaria. Malaria control programs were abandoned because they were ineffective, there was no effective vector control, and access to treatment was limited, in addition to the declining efficacy of chloroquine, the most commonly used antimalarial at that time. During this period, hundreds of millions of people were infected with malaria, and tens of millions died from it, mainly in the sub-Saharan Africa. It took three decades for malaria to re-emerge as a public health control priority worldwide and the discussion about the barrier to socio-economic development to reopen (World Health Organization, 2020).

This situation led to important political events in the 1990s that helped shape the first two decades of the 21$^{st}$ century, the golden era in the history of malaria control. This renewed political commitment and the growing availability of better tools to fight the disease contributed to the signing of the Abuja Declaration in April 2000, aiming to cut by half the malaria mortality for Africa's people by 2010, with more access to effective treatment and protection with insecticide-treated mosquito nets (ITNs). In September 2000, the eight Millennium Development Goals (MDGs) were launched, with a clear articulation that malaria was a global development issue and appealing the end of the malaria epidemy, which reinforced the Abuja Declaration (World Health Organization, 2020).

Throughout these 20 years, several efforts were made to reduce the burden of malaria and eliminate the disease. In 2000, in response to reduced efficacy to chloroquine, the use of ACTs was recommended by WHO, as well as approved the first long-lasting insecticide nets (LLIN). In 2002, the Global Fund to fight AIDS, Tuberculosis, and Malaria was established, marking the beginning of an unprecedented period for malaria funding. In 2005, the Innovative Vector Control Consortium (IVCC) was established to respond to the threat of insecticide resistance. Finally, in 2015, the WHO Global technical strategy (GTS) for malaria 2016-2030 was launched, including three pillars: to ensure universal access to malaria prevention, diagnosis, and treatment; to accelerate efforts towards elimination and attainment of malaria-free status; and to transform malaria surveillance into a core intervention (World Health Organization, 2020).

Nevertheless, the GTS 2020 milestones for morbidity and mortality will not be achieved globally. The projections present in the GTS report took into account the 2000-2019 malaria trends. Therefore, there is a deceleration in the rate of decline in case incidence and mortality, being the first one 37% off track and the second one 22%. Although significant efforts are being made to contradict this rate slowing,

resistance to first-line treatments, among other biological threats, is threatening GTS's achievement (World Health Organization, 2020).

## 1.3. Malaria Infection Biology

Malaria is caused by a parasitic infection with unicellular protists of the *Plasmodium* genus (Josling & Llinás, 2015), transmitted through an infected female *Anopheles* mosquito (Pannu, 2019). There are six *Plasmodium* species known to infect and transmit from humans, *P. falciparum*, *P. vivax*, *P. ovale curtisi*, *P. ovale wallikeri*, *P. malariae,* and *P. knowlesi* (Ashley & Phyo, 2018). This last one is a zoonotic species, which infects mainly monkeys; however, human infections have been encountered in Southeast Asia (Plewes et al., 2019). In addition, there are other zoonotic species, such as *P. chabaudi*, which infects rodents and is used as an *in vivo* model to study malaria (Stephens et al., 2012), being an essential research tool since it is a robust model system for identifying genetic loci, candidate genes and individual mutations underlying drug resistance (Hunt et al., 2007).

*Plasmodium* spp. has a complex biological life cycle, resulting in a high degree of cell and clinical variability. An important variance is the existence of parasite latency forms, such as hypnozoite present in *P. vivax* and *P. ovale* species, which can reinitiate infection months or years later (Ross & Fidock, 2019).

*Plasmodium* infections result in a wide spectrum of clinical outcomes, going from acute febrile illness to life-threatening organ dysfunction affecting the brain, lungs, liver, and kidney, causing metabolic acidosis, respiratory distress, cerebral malaria, coma, or death (Pannu, 2019; Ross & Fidock, 2019). The most severe clinical features are usually associated with *P. falciparum*, mainly due to its ability of cytoadherence (Plewes et al., 2019), being responsible for 95% of all malaria deaths (Moxon et al., 2020). Additionally, *P. falciparum* and *P. vivax* represent the most significant threat accounting for most cases worldwide (World Health Organization, 2020).

## 1.4. *Plasmodium falciparum*

*P. falciparum* parasites have a complex life cycle, alternating between two hosts, human where the asexual multiplication occurs and mosquitos where the sexual phase occurs, allowing the transmission to the next human host (Josling & Llinás, 2015).

The human infection begins when an infected female *Anopheles* mosquito deposits approximately 100 sporozoites into the skin and vasculature during a blood meal. From the bloodstream, sporozoites migrate to the liver and invade hepatocytes, where they replicate over a week, resulting in an estimated 10,000-30,000 merozoite progeny per intracellular parasite. These merozoites are released into the bloodstream, where they invade mature erythrocytes and develop a parasitophorous vacuole. In this blood stage of infection, parasites undergo repeated ~48h cycles of asexual growth, egress, and reinvasion. In this cycle, parasites pass through ring, trophozoite, and schizont stages, which replicate into new merozoites that are released and infect new red blood cells (RBCs). These repeated cycles result in a multiplication of parasites and lead to clinical symptoms, including spikes of fever (Blasco et al., 2017; Krishnan & Williamson, 2018; Sato, 2021; Zekar & Sharman, 2020).

A small proportion of merozoites, approximately 1-2%, start an alternative program of sexual development, which lasts for 10-12 days. These parasites differentiate into male and female gametocytes that reach the host's dermis. During a blood meal, about $10^3$-$10^4$ mature gametocytes are ingested by a mosquito, where they undergo the sexual phase of the life cycle, forming male and female gametes ($10^2$-$10^3$). After ingestion, the male micro-gametocytes go through a process of ex-flagellation in the mosquito's midgut, fusing with female macro-gametes to form zygotes. The zygote undergoes meiosis and differentiates into ookinetes (<100), which migrate through the wall of the mosquito midgut and mature into oocysts (typically 1-2). About $10^3$-$10^4$ sporozoites are produced in the oocyst. Upon rupturing, sporozoites are released and dispersed through mosquitos bodies, including salivary glands, where they acquire the ability to infect new human hosts, therefore completing the life cycle (Blasco et al., 2017; Krishnan & Williamson, 2018; Sato, 2021; Zekar & Sharman, 2020).

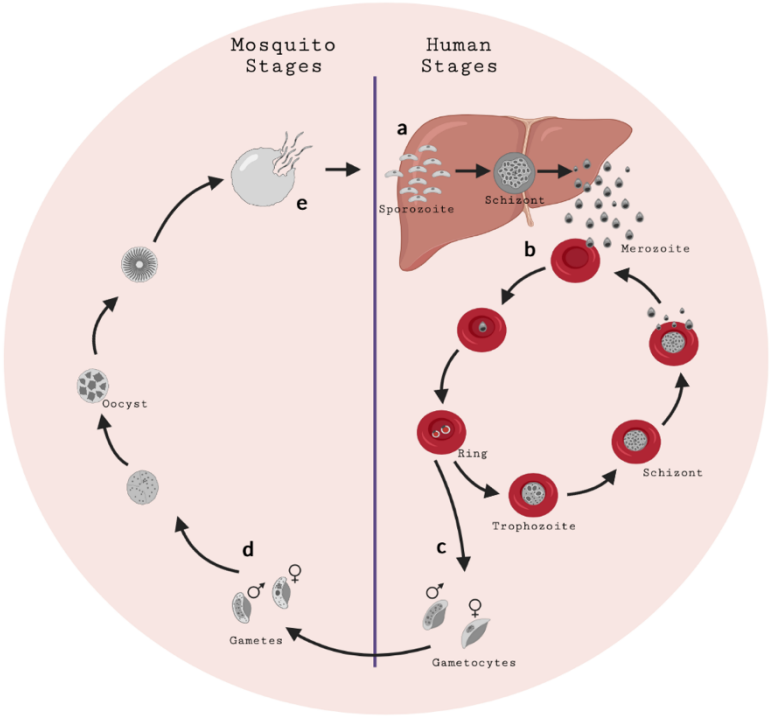


**Figure 2.** ***Plasmodium falciparum*** **life cycle. (a)** Human infection begins when an infected female *Anopheles* mosquito, during a blood-feeding, delivers sporozoites into the dermis and bloodstream of the human host, migrating to the liver, where they invade hepatocytes and replicate, resulting in merozoites. **(b)** These merozoites are released into the bloodstream and invade mature RBCs, where they initiate ~48h cycles of asexual replication, passing through ring and trophozoite stages, and finally schizont, where merozoites are formed and released to invade new RBCs. **(c)** A small proportion of merozoites differentiate into mature male and female gametocytes that are posteriorly transmissible to *Anopheles* mosquitoes. **(d)** During a blood meal, mature gametocytes are taken up by the mosquito and form male and female gametes, which undergo sexual recombination, forming ookinetes and then oocysts, **(e)** which will lead to the formation of sporozoites, that migrate to salivary glands, ready to reinitiate human infection. Adapted from Antimalarial drug resistance: Linking Plasmodium falciparum parasite biology to the clinic (Blasco et al., 2017).

As mentioned before, *P. falciparum* is the most virulent species capable of infecting humans due to its ability to promote erythrocytes adhesion to the microvascular endothelium (cytoadherence) through surface modifications of the host RBCs, exporting and presenting variant surface antigens (VSA). In *P. falciparum*, three major VSA families have been identified, *P. falciparum* erythrocyte membrane protein 1 (*Pf*EMP1) encoded by the *var* genes (Milner, 2018), repetitive interspersed repeats (RIFIN) encoded by the *rif* genes, and subtelomeric variant open reading frame (STEVOR) encoded by the *stevor* genes (Yam & Preiser, 2017). It causes a considerable obstruction to tissue perfusion and, consequently, evades clearance through the immune system (Belachew, 2018; Josling & Llinás, 2015; White, 2017).

## 1.5. Antimalarials

Antimalarial drugs have been the main form of control and treatment of malaria. Since ancient times, various plant products have been used to treat malaria. In 1820, quinine was isolated from cinchona, one of the most effective treatments to date (Cowman et al., 2016; Sato, 2021). However, resistance to quinine was reported in the 1980s, and it is no longer used as a front-line treatment. In the twentieth century, after efforts to chemically synthesize pure compounds, several other synthetic compounds have been developed, such as mepacrine, chloroquine, mefloquine, and halofantrine. Mepacrine, a derivative of methylene blue, was predominantly used throughout the Second World War but it is no longer used due to the emergence of undesirable side effects. Chloroquine was the major antimalarial used in the twentieth century, but, over the years, many strains of malaria have developed resistance, being the first one reported in the 1950s. Mefloquine was developed in the 1970s and, despite resistance first reported in 1986, it is still used today (although not widely), mostly in combination with a complementary drug. Halofantrine was developed between the 1960s and 1970s in order to combat all forms of *Plasmodium* parasites, though its use has been reduced due to undesirable side effects (Tse et al., 2019).

In 1972, another natural compound, artemisinin, was isolated from *Artemisia annua*, a herb commonly used in traditional Chinese medicine and reported antimalarial properties (Sato, 2021; Tse et al., 2019; Tu, 2016). Pharmacological and clinical studies showed that artemisinin has a rapid onset of action, low toxicity, and efficacy against both drug-resistant and dug-sensitive malaria, poor solubility in water or oil and a high rate of parasite recrudescence. Taking these shortcomings into account, the chemical structure and activity were studied, founding dihydroartemisinin (DHA), a more active form than artemisinin but still with poor solubility and lower stability (Y. Li, 2012). Therefore, semi-synthetic derivatives were synthesized, with artemether, artesunate, and arteether being the most common derivatives, which are prodrugs transformed to the active metabolite, dihydroartemisinin (Tse et al., 2019). The impact of this drug in the reduction of infection and death in malaria led to the awarding of part of the Nobel Prize in 2015 in Medicine to TU You-You of the China Academy of Traditional Chinese Medicine (LU et al., 2019).

Nowadays, five classes of antimalarial drugs are used in the clinical treatment of human malaria based on their structural backbone and action. The classes are: (1) endoperoxides (artemisinin and its derivatives) - the most widely used; (2) 4-aminoquinolines (chloroquine), aryl-amino alcohols (quinine, mefloquine); (3) antifolates (pyrimethamine, proguanil, sulfadoxine); (4) naphthoquinones (atovaquone); and (5) 8-aminoquinolines (primaquine, tafenoquine). The 4-aminoquinolines, aryl-amino alcohols,

antifolates, and naphthoquinones' main inhibition targets are the detoxification of heme released upon hemoglobin degradation. On the other hand, endoperoxides act in multiple cellular processes, yielding free radicals in the parasite cells (Sato, 2021).

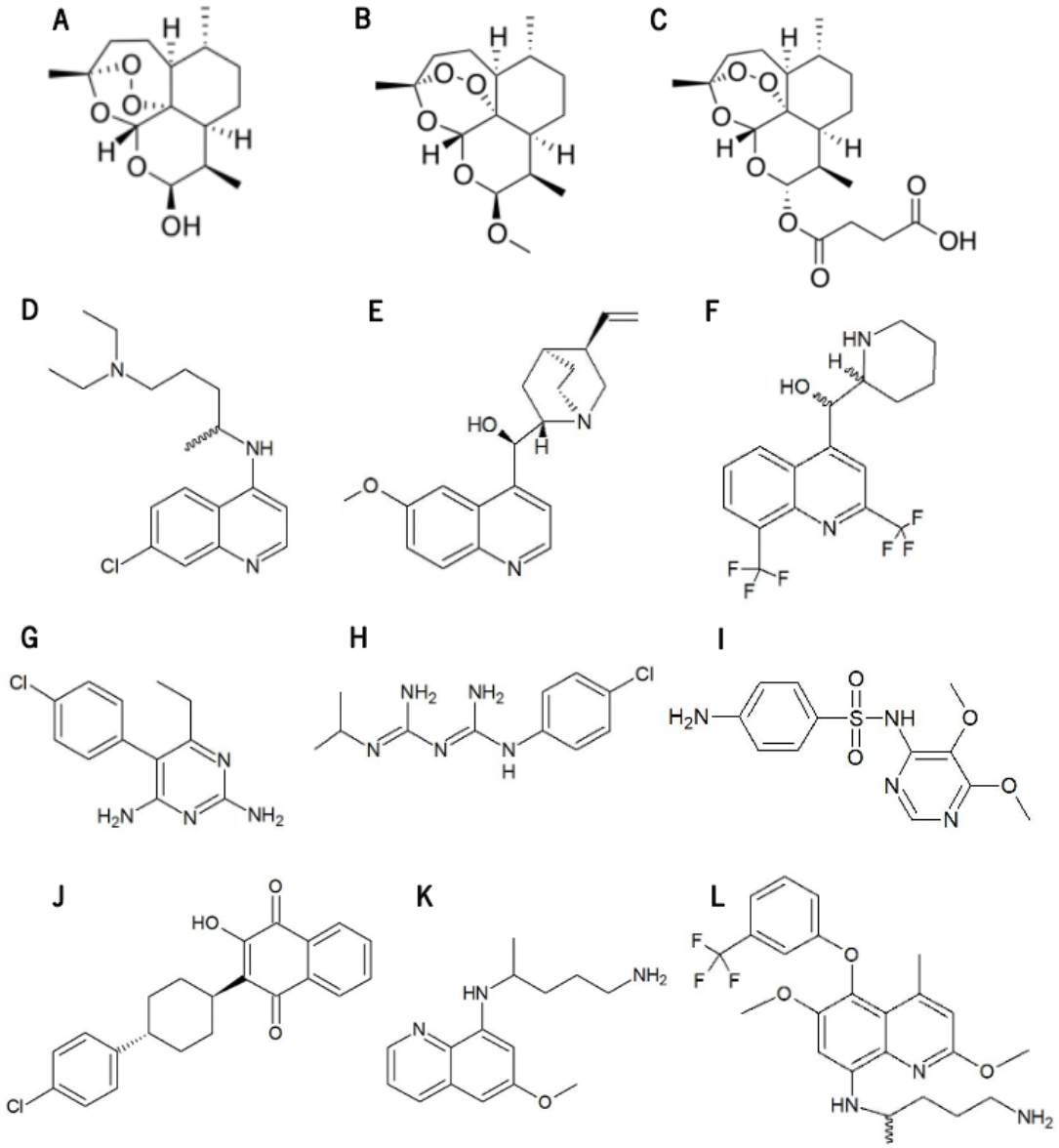


**Figure 3. Antimalarials classes.** (1) Endoperoxides: **(A)** Dihydroartemisinin, **(B)** Artemether, **(C)** Artesunate. (2) 4-aminoquinolines: **(D)** Chloroquine; Aryl-amino alcohols: **(E)** Quinine, **(F)** Mefloquine. (3) Antifolates: **(G)** Pyrimethamine, **(H)** Proguanil, **(I)** Sulfadoxine. (4) Naphthoquinones: **(J)** Atovaquone. (5) 8-aminoquinolines: **(K)** Primaquine, **(I)** Tafenoquine.

### 1.5.1. Artemisinin

Nowadays, artemisinin and its derivatives (ARTs) are the recommended course of treatment for uncomplicated malaria by WHO (Davis et al., 2020). It exerts potent activity against the intraerythrocytic asexual *Plasmodium* blood stage. It first needs to be activated by the cleavage of its endoperoxide bridge upon reaction with FeII-heme, which becomes accessible with the hemoglobin degradation. This degradation occurs due to the parasite's need to consume hemoglobin in order to generate protein-building blocks and to create space for growth (Xie et al., 2020). ARTs are lethal to parasites in this activated state, presumably due to their reaction with susceptible groups in biomolecules, including heme, proteins, and lipids, causing oxidative stress and cellular damage (Blasco et al., 2017; Talman et al., 2019). However, other possible mechanisms of action were shown in recent studies, as the demonstration that artemisinin inhibits *P. falciparum* phosphatidylinositol-3-kinase (*Pf*PI3K), which catalyzes the production of phosphatidylinositol-3-phosphate (PI3P), which is involved in the protein retention in the *P. falciparum* endoplasmic reticulum (ER) (Mbengue et al., 2015). Decreased levels of PI3P lead to increased exportation of parasite proteins, mediating the virulence to the erythrocyte (Bozdech et al., 2015).

Artemisinin reduces the parasite load up to 10 000-fold in a single erythrocytic multiplication cycle (48h), providing rapid clearance rates. Therefore, a 7-day treatment plan is necessary for a complete cure when taken as monotherapy (Ferreira et al., 2013). However, they are rapidly metabolized, with a half-life of 1-2h, being necessary to add a longer-lasting partner drug to eliminate infections (Blasco et al., 2017; Talman et al., 2019).

ACTs, the combination of an ART derivative with a longer-lasting partner drug, assures sustained antimalarial pressure after the rapid reduction of the parasite biomass induced by the endoperoxide, increasing the treatment efficacy and reducing the selective pressure for resistance (Eastman & Fidock, 2009). Furthermore, a 3-day course of the artemisinin component of ACTs ensures that only a small number of parasites remain for clearance by the partner drug. There are several combinations of ACTs, being the leading ones in use nowadays: artemether-lumefantrine, artesunate-amodiaquine, dihydroartemisinin-piperaquine artesunate-mefloquine, artesunate plus sulfadoxine-pyrimethamine, and artesunate-pyronaridine (Ashley et al., 2018; Rosenthal & Ng, 2020).

## 1.6. Resistance

### 1.6.1. Artemisinin-based Combination Therapies (ACTs) Resistance

The loss of first-line malaria treatments for resistance has been a constant struggle in controlling this disease. The ability of *P. falciparum* to develop resistance has threatened their efficacy and stimulated the development of new drugs and the use of combinations. After the spread of parasite resistance to chloroquine and other antimalarials, ACTs were recommended for treatment (Cowman et al., 2016). However, in the late 2000s, there were reports from Cambodia of decreased sensitivity to artemisinin derivatives (Dondorp et al., 2009; Noedl et al., 2008), being now detected across the Greater Mekong Subregion (GMS), in Equatorial Guinea and Uganda, which is of particular concern because the Sub-Saharan Region of Africa is where malaria exerts its most significant burden (LU et al., 2019). Cases from South America were also reported (Douine et al., 2018; Vreden et al., 2013).

Unlike other antimalarial drugs where resistance is defined as clinical treatment failure and reduced *in vitro* sensitivity (Ferreira et al., 2013; LU et al., 2019), artemisinin resistance is characterized by parasites that display clearance times greater than three days or parasite clearance half-lives greater than five hours after treatment with artemisinin or ACTs (Rosenthal & Ng, 2020), demonstrating increased survival rates (LU et al., 2019).

Artemisinin resistance appears to be mediated by different genetic loci in parasites of distinct regions. Nonetheless, resistance mechanisms are frequently associated with alterations in hemoglobin uptake, hemoglobin digestion, antioxidant response, DNA repair, and cell stress pathways (Rosenthal & Ng, 2020).

### 1.6.2. Resistance Mechanisms associated with K13 mutations

Artemisinin resistance has been frequently associated with polymorphisms in the β-propeller domain *P. falciparum* Kelch 13 (*Pf*K13) propeller protein, encoded by the *pfk13* locus (Ashley et al., 2014; LU et al., 2019; Sutherland et al., 2020). Parasites with these mutations present alterations in the intraerythrocytic cell cycle, such as lengthened ring stage and shortened trophozoite stage, in addition to modifications at the molecular level, as a higher expression of unfolded protein response pathways, decreased levels of ubiquitinated proteins, as well as of *Pf*K13 protein, and phosphorylation of the parasite eukaryotic factor-2α (eIF2α) during the early intraerythrocytic stage, which is responsible for the arrest of protein translation and, consequently, ART-induced dormancy (Coppée et al., 2019). Nevertheless, the exact mechanism by which Kelch-13 protein induces ART resistance remains unclear (Xie et al., 2020).

K13 is a 726 amino acid protein, which comprises three domains: a conserved *Plasmodium*-specific N-terminal domain, a putative BTB/POZ domain (Broad complex_Tramtrack_bric-a-brac/Pox virus_Zinc finger), and a C-terminal domain containing six Kelch motifs, which forms a six-bladed β-propeller (Tilley et al., 2016). It has sequence similarity to a class of Kelch/BTB/POZ ubiquitination adaptors and may be involved in binding to cullin 3, the largest family of E3 ubiquitin ligases, orienting to specific substrates (Tilley et al., 2016; Xie et al., 2020).

K13 has been localized in cytostomes at the parasite periphery and in intracellular vesicles, associated with endocytosis or vesicular trafficking of antigens, like *Pf*EMP1 or Rab-mediated protein transport. As mutations in the *pfk13* locus decrease K13 levels, it leads to reduced hemoglobin endocytosis and catabolism in young rings, which results in decreased levels of free Fe(II)-heme available to activate artemisinin (Wicht et al., 2020). The same outcome is observed when K13 is mislocalized in early ring-stage parasites, decreasing hemoglobin-like peptides (T. Yang et al., 2019). These mutations have also been proposed to deregulate the activation of *Plasmodium* eIF2α kinase, PK4, as a response to cellular stress, leading to the phosphorylation of eIF2α and inhibiting general protein synthesis (Wicht et al., 2020; M. Zhang et al., 2017). As a result of the reduced hemoglobin endocytosis and the phosphorylation of eIF2α the parasite promotes latency and confers an extended period of ring-to-trophozoite stage development (Wicht et al., 2020).

As mentioned before, artemisinin presumably kills parasites with an accumulation of cellular damage and oxidative stress, being responsible for disrupting the proteasome-dependent degradation, in addition to the alkylation of biomolecules (Bridgford et al., 2018). Therefore, a mechanism to maintain the protein turnover would be essential to assure survival towards ARTs action. One hypothesis was that K13 mutations removed damaged proteins by upregulating the unfolded protein response (UPR) and enhancing their cell stress response by maintaining the ubiquitin-proteasome system (UPS) (Dogovski et al., 2015; Mok et al., 2015; Wicht et al., 2020). The UPR upregulation, which may be due to the loss of function of K13, which is a negative regulator of this pathway (Digaleh et al., 2013), leading to the constitutive activation at baseline, presumably increases the ability of parasites to rapidly repair or degrade biomolecules damaged by short exposures to artemisinin. The *Plasmodium* Reactive Oxidative Stress Complex (PROSC) and tailless complex polypeptide (TCP)-1 Ring Complex (TRiC) chaperonin complexes may be involved in this process since they play that role in other eukaryotes. This upregulation may also be linked with decelerated parasite development (Mok et al., 2015), along with the eIF2α phosphorylation.

Regarding the enhanced cell stress response by maintaining the UPS, synergy between artemisinin and proteasome inhibitors has been observed (Dogovski et al., 2015). However, it has been observed in both K13 mutants and wild-type parasites, which showed that K13 mutations do not modulate proteasome activity. Therefore, one alternative to protect against ART's proteolytic activity is the reduced drug binding to and polyubiquitination of PI3K, increasing the levels of PI3P vesicles, which are involved in cellular processes, such as protein folding, vesicle-mediated protein export, and the UPR (Wicht et al., 2020). Furthermore, it may also be implicated in the regulation of autophagy, with the modulation of the levels of PI3P, which is involved in autophagosome formation, helping to remove damaged proteins (Ng et al., 2017).

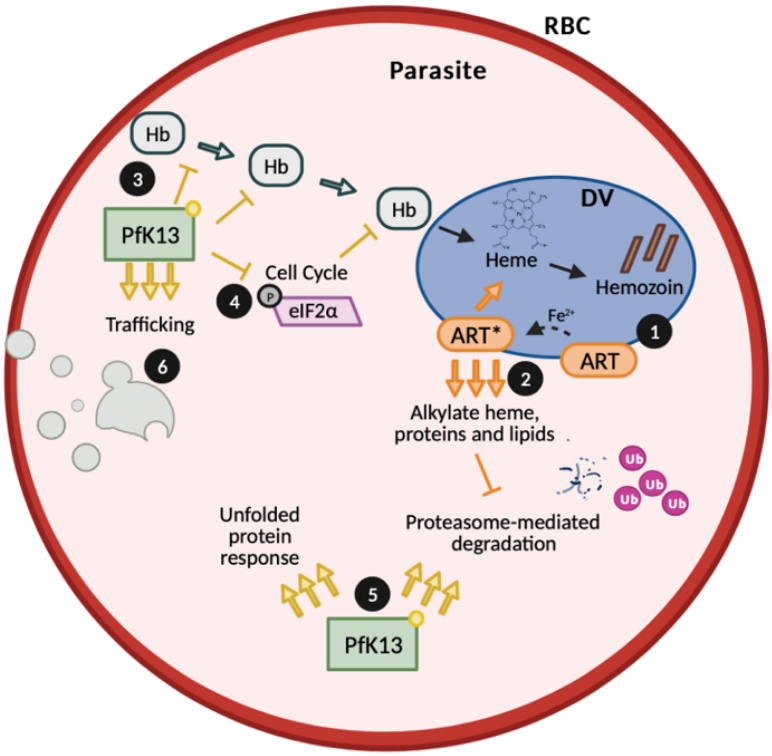


**Figure 4. K13-mediated mechanism of action and resistance of artemisinin in *P. falciparum* intraerythrocytic stage. 1.** ARTs are activated with the cleavage of the endoperoxide bridge after reaction with the product of parasite-digested hemoglobin, Fe(II)-heme; **2.** After activation (represented by ART*), artemisinin alkylates and damages parasite proteins, heme, and lipids, and inhibits proteasome-mediated protein degradation. **3.** K13 mutations confer artemisinin resistance. The loss of its function causes reduced endocytosis of host hemoglobin and **4.** extends the ring-stage development duration, presumably through eIF2α phosphorylation mediated by PK4, resulting in reduced levels of hemoglobin catabolism and, consequently, the availability of Fe(II)-heme, leading to decreased activation of ARTs. **5.** K13 mutations may also increase the unfolded protein response, maintain proteasome-mediated degradation of polyubiquitinated protein,s and **6.** remove drugs and alkylated proteins by increasing PI3K-mediated vesicular trafficking. Adapted from Molecular Mechanisms of Drug Resistance in *Plasmodium falciparum* Malaria (Wicht et al., 2020).

## 1.7. Proteasome

### 1.7.1. Proteasome Structure

The UPS is essential to eukaryotic cells as it is responsible for the degradation or recycle of proteins, influencing several cellular processes, including cell cycle, transcriptional regulation, cellular stress response, signal transduction, and cellular trafficking (Wang et al., 2015). This protein regulation is critical for the rapid transformations that malaria parasites suffer during the life cycle progression between the two hosts, especially in the stages with high replication rates (Krishnan & Williamson, 2018). The ubiquitin-proteasome pathway (UPP) involves a posttranslational modification protein, called ubiquitination, which attaches proteins to a polyubiquitin chain that is subsequently recognized by the 26S proteasome. The type of ubiquitination defines if the protein is recycled or degraded by the proteasome (Aminake et al., 2012; Wang et al., 2015).

The conjugation of ubiquitin to biomolecules is controlled and gradually. It starts with the ubiquitin being proteolytically processed to reveal a diglycine motif by ubiquitin-specific proteases (USPs), followed by ubiquitin binding to the ubiquitin-activating enzyme (E1) cysteine active site, an ATP-dependent step. Active ubiquitin is then transferred to the ubiquitin-conjugating enzyme (E2). This activated intermediate of E2-ubiquitin functions as the ubiquitin donor to the ubiquitin ligase (E3), which binds both the substrate and the mediator through different structural motifs, transferring the ubiquitin from the E2 to the substrate. The ubiquitin chains may be elongated via ubiquitin chain-elongation enzyme (E4) or by the same E3. These ubiquitin chains are posteriorly recognized by the proteasome and removed from the substrate by the deubiquitinases (DUBs), whereas substrates are cleaved into short peptides and posteriorly broken down to amino acids by aminopeptidases (APPs). Finally, released polyubiquitin molecules are recycled by cytosolic DUBs for another round of ubiquitylation (Mao, 2021; Ng et al., 2017).

The 26S proteasome, a barrel-shaped multi-subunit proteinase complex, is divided into a 20S core particle (CP) and a 19S regulatory particle (RP). This latter is responsible for the recognition, deubiquitination, unfolding, and translocation of substrates. The 20S core is responsible for proteolysis via peptidylglutamyl-peptide hydrolytic (PGDH) (caspase-like), trypsin-like, and chymotrypsin-like activities, encountered in three β-subunits (β1, β2, and β5, respectively) (Wang et al., 2015). These catalytically active subunits use a N-terminal threonine as the nucleophile and cleave after the carboxy-terminal side of acidic, tryptic, and hydrophobic residues, respectively. These active sites are located in the two inner beta rings of the barrel, consisting of β1-β7, while the two outer rings consist of α1-α7, which prevent

polypeptide access to the catalytic subunits. This gate opening of the 20S core is regulated by the 19S subunits (H. Li et al., 2016; Ng et al., 2017).

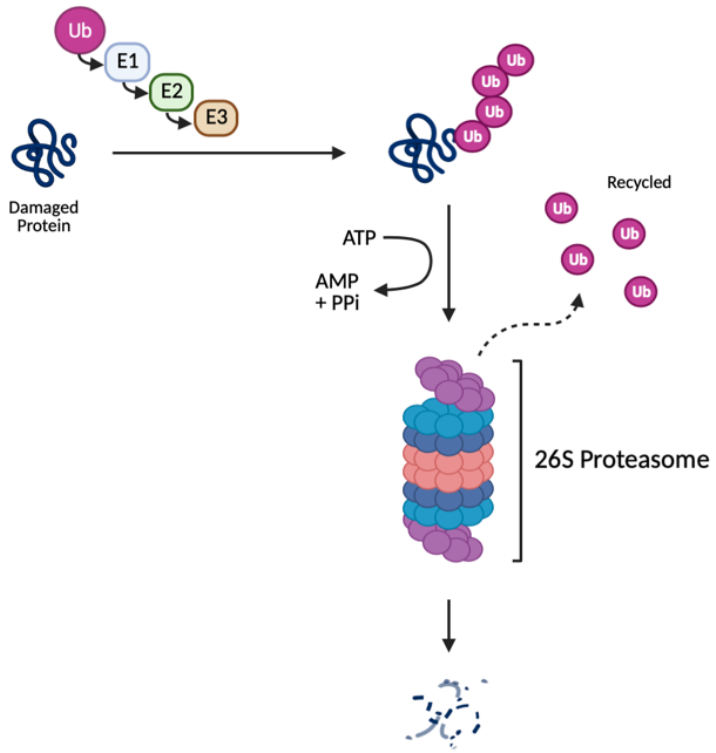


**Figure 5. The ubiquitin-proteasome pathway.** Damaged biomolecules are attached with a polyubiquitin chain, via the ubiquitin-activating enzyme (E1), ubiquitin-conjugating enzyme (E2), and ubiquitin ligase (E3), being posteriorly recognized by the 19S RP of the 26S proteasome and presented to the 20S CP, responsible for the degradation of biomolecules and recycling of ubiquitin molecules. Adapted from Advances in the Understanding of Mechanisms and Therapeutic Use of Bortezomib (Mujtaba & Dou, 2011).

The 19S RP consists of at least 18 protein subunits, structurally divided into two subcomplexes, lid and base. The lid subcomplex comprises nine regulatory particle non-ATPase (rpn) subunits (3, 5, 6, 7, 8, 9, 11, 12, 15), while the base subcomplex includes the other rpn and six paralogous distinct regulatory particle ATPase (rpt) subunits. These last ones are responsible for the protein unfolding and the CP gate opening, being necessary insertion of the C-terminal of all rpt subunits except rpt4 into the external pockets of the α-ring to open. In addition, they also stabilize the interaction of the 19S RP with the 20S CP (Mao, 2021).

The first step of substrate processing by the proteasome is recognizing a ubiquitylated substrate, mediated by the ubiquitin receptors within the base, including rpn1, rpn2, rpn10, and rpn13. Rpn10 attaches to the central solenoid portion of rpn1, being this ligation stabilized by the presence of rpn2, where the rpn13 subunit will bind. In addition to these ubiquitin receptors, ubiquitylated substrates can also be recruited and delivered to the proteasome by extrinsic receptors, ubiquitin-like (UBL), and ubiquitin-associated (UBA) domains. These UBL-UBA proteins interact with the intrinsic ubiquitin-binding sites through their UBL domain, functioning as shuttle factors that diversify the routes of decoding the ubiquitin signals for substrate selection and recognition. Rpn1 and rpn2, the two largest proteasome subunits, function as scaffolds and coordinate the activity and placement of multiple ubiquitin-processing factors at the proteasome. In these subunits, the UBL recognition sites prioritize the binding partners and place them in the context of competing with the ubiquitin-binding (Mao, 2021; Rosenzweig et al., 2012).

### 1.7.2. 26S Proteasome and Artemisinin Resistance

As mentioned before, there is potent synergy between DHA and proteasome inhibitors, regardless of the K13 genotype, both *in vitro* and *in vivo*. DHA generates carbon-centered radical species, which non-specifically alkylate intracellular heme and other biomolecules in blood-stage parasites, increasing the burden of misfolded and damaged proteins. These biomolecules accumulate as UPS substrates. Therefore, inhibition of the *P. falciparum* proteasome prevents parasites from resolving protein damage caused by these compounds, creating the synergy between the drugs (Stokes et al., 2019).

Transcriptomic analyses of clinical isolates from the Tracking Resistance to Artemisinin Collaboration (TRAC) demonstrated that resistant parasites, in addition to upregulate protein folding chaperones and DNA damage responsive genes, also upregulates components of the proteasome (Mok et al., 2015). This implicates that UPP is involved in ART action and resistance. In addition, mutations in ubiquitination machinery have been reported to be associated with ART resistance. Furthermore, inhibiting polyubiquitination antagonizes DHA activity, confirming that DHA requires the accumulation of polyubiquitinated proteins for malaria treatment (Bridgford et al., 2018; Hunt et al., 2007). A recent study also demonstrated that a mutation in the β2 subunit of the 20S core sensitized $K13^{C580Y}$ parasites, the most prevalent mutation in the GMS region, to DHA (Rosenthal & Ng, 2021).

## 1.8. Context and Objectives

Malaria parasites increasingly develop resistance to all drugs available in the market, hampering the goal of reducing the malaria burden and deaths (Antony & Parija, 2016). Therefore, it is crucial to understand the mechanisms by which parasites gain resistance to antimalarials to develop better treatments in the future. As mentioned before, artemisinin resistance has been associated with mutations in the K13 protein, which do not modulate proteasome activity (Wicht et al., 2020). However, using a proteasome inhibitor, such as epoxomicin, intensifies artemisinin activity in resistant and sensitive parasites (Bozdech et al., 2015). On that account, mutations in different parts of the ubiquitin-proteasome pathway may impact the artemisinin response (Bridgford et al., 2018).

In a collaboration, GHTM/IHMT/Universidade Nova de Lisboa, the genome of ACT resistant *P. chabaudi* parasites, in this case, artesunate and mefloquine, was investigated for the presence of associated mutations. As a result, a single-nucleotide variant (SNV), E738K, in the 26S proteasome regulatory subunit *rpn2* gene was found, and it was shown, considering the rpn2 tertiary structure, to alter their protein's network interactions, since a glutamic acid (E), a negative polar amino acid, is replaced for lysine (K), a positive polar amino acid (unpublished data). Therefore, this project aimed to evaluate the impact of the E738K in the proteasome function and response to artemisinin in *P. falciparum* parasites and, consequently, give further knowledge of the role of the UPP in the artemisinin response and resistance.

# 2. Materials and Methods

## 2.1. Cloning strategy

DNA sequences were obtained using the database PlasmoDB (www.plasmodb.org). *P. chabaudi* gene ID is PCHAS_133430 and *P. falciparum* is PfDd2_140070600. Cloning strategies were designed *in silico* with the software Ape.

### 2.1.1. *P. falciparum* and *P. chabaudi* gDNA extraction

*P. falciparum* genomic DNA (gDNA) was extracted from a Dd2 parasite culture, while *P. chabaudi* gDNA was obtained from a blood sample of infected mice from the collaborator GHTM/IHMT. Both samples were extracted using the NZY Blood gDNA isolation (NZYTech). Afterward, concentration and purity were measured using NanoDrop™ 1000 spectrophotometer (Thermo Scientific), and the gDNA was stored at -20°C.

### 2.1.2. Fusion

To construct a plasmid with parts from both species, the Selection-Linked Integration (SLI) technique was used. For that, the regions of interest of each species were amplified through a Polymerase Chain Reaction (PCR). Primers were designed taking into account the gene sequence, being the reverse primer from *P. falciparum* (p431) and the forward primer from *P. chabaudi* (p432) similar, due to the similarities between both sequences and to allow subsequent fusion (Table 1). To each PCR, 200 ng/µL of template, 0.5 µM of each primer, 200 µM dNTPs, 0.02 U/µL iProof DNA polymerase and respective buffer, 5X iProof High-Fidelity (HF) Buffer (Bio-Rad Laboratories) was added. After 5 min at 95°C to denature the template DNA, 35 cycles were initiated, consisting of 94°C for 30 sec, 60°C for 30 sec and 72°C for 30 sec to *P. falciparum* 45 sec to *P. chabaudi*. After 5 min at 72°C to the final extension, it culminates at 4°C until the tubes are collected. Samples were analyzed by electrophoresis in an agarose gel (1%), using a molecular weight marker (GeneRuler 1kb DNA Ladder, Thermo Fisher Scientific) to confirm that the obtained fragments had the expected size.

Table 1. Primer sequences used for plasmid construction and genotyping.

| Name | Primer Sequence (5'→3') | Tm |
|---|---|---|
| p430 | ACTCGCGGCCGCTAAGAAAATGAAAGTAATGCAATAACGA | 69°C |
| p431 | TATCATGTGCATATGCTAGCAATTCGTCTATACATTTATC | 62°C |
| p432 | TATAGACGAATTGCTAGCATATGCaCATGATACACAACAT | 64°C |
| p433 | TTTGAGCCCTTTACTTGGAAAGATGAAAACGTCGACGGAG | 68°C |
| p483 | GATACACAACATGAAAAAATAACAAGAGCATGTAGTATA | 60°C |
| p484 | GTTATTTTTTCATGTTGTGTATCATGTGCATATGCTAGC | 62°C |
| p39 | TATCGTTACGTCCGCCAGTG | 58°C |
| p40 | CTCCTGCACAAGTTCCAATG | 55°C |

Other PCR was performed to fusion both fragments. The forward primer of the *P. falciparum* part (p430) and the reverse primer of the *P. chabaudi* part (p433) were used. iProof HF DNA Polymerase (Bio-Rad Laboratories) was used again. The reaction was similar to the one previously described, differentiated only in the annealing temperature, which was 55°C and in the number of, having decreased to 18 cycles. As previously, the sample size was analyzed by electrophoresis. The correct band was then extracted using GRS PCR & Gel Band Purification kit (GRiSP, Lda).

### 2.1.3. Selection-Linked Integration

The previous product was posteriorly inserted in the JET plasmid (CloneJET PCR Cloning kit, Thermo Fisher Scientific). This step was performed to store the PCR product in a stable vector, avoiding the need to repeat all the previous steps in the event of something not working. Since the PCR product has blunt extremities, ligation to the vector was performed, considering the protocol indicated for these products in the kit.

The above ligation reaction products were then transformed into chemically competent *Escherichia coli* cells (XL-10) by heat shock. This is a physical method of transformation, which consists of a rapid difference in temperature, generating a pressure difference between the interior and exterior of the host cells, which in turn induces the formation of pores in the plasma membrane of the bacteria, allowing entry of the plasmid in cells. Next, *E. coli* cells were placed on ice for 15 min for thawing, followed by adding the plasmid (10% of *E. coli* cells volume) and incubated on ice for 20 more min. Afterward, to proceed with the thermal shock, they were placed at 42°C for 40 sec on a thermoblock, followed by 2

min on ice. Subsequently, 300 µL of Super Optimal broth with Catabolite repression (SOC) medium [20 g/L bacto-tryptone, 5 g/L bacto yeast extract, 10 mM NaCl, 2.5 mM KCl, 0.1M $MgCl_2$, 10 mM $MgSO_4$, and 20 mM glucose] was added and the cells recovered for 1 hour at 37°C with shacking, at 200 rotations per min (rpm). Posteriorly, cells were transferred to lysogeny broth (LB) medium [10 g/L bacto-tryptone, 5 g/L yeast extract, and 10 g/L NaCl] plaques supplemented with ampicillin antibiotic (100 µg/mL) and incubated overnight at 37°C. The choice of this antibiotic for the selection of transformed cells is because the pJET vector contains a cassette for its resistance. The next day, two of the emerged colonies were picked up into 5 mL of LB medium with ampicillin (100 ug/mL) to grow overnight. Plasmids were extracted using the Zyppy™ Plasmid Miniprep Kit (Zymo Research). After that, concentration and purity were measured using NanoDrop™ 1000 spectrophotometer (Thermo Scientific). Finally, to assess the plasmid correctness, it was sent for sequencing.

Subsequently, the fragment was inserted in the Selection-Linked Integration plasmid (pSLI), being first needed to digest both the pSLI (Addgene) and the fragment with NotI (New England Biolabs) and SalI (New England Biolabs). Electrophoresis was used to verify the digestion with an agarose gel (1%) and a molecular weight marker (GeneRuler 1kb DNA Ladder, Thermo Fisher Scientific), and the desired bands were extracted with the GRS PCR & Gel Band Purification kit (GRiSP, Lda). Then, ligation of the fragment to the plasmid was carried out. The ligase used was T4 DNA Ligase (Thermo Fisher Scientific).

After inserting the fragment into the pSLI, the construct was transformed into competent *E. coli* cells by heat shock as previously and transferred to LB plates containing ampicillin (100 µg/mL). The plates were left overnight in an incubator at 37°C, and, on the second day, a colony was picked into 5 mL of LB medium with ampicillin (100 µg/mL) to grow overnight. The following day, plasmid extraction from the liquid culture containing the transformed cells was performed using the NZYMiniprep kit (NZYTech, Lda.). To verify if the colony had the correct plasmid, genotyping was performed using the PvuII enzyme (New England Biolabs), which generated a proper pattern for the colony with the plasmid containing the fragment. After that, it was sent to sequencing.

### 2.1.4. Site-Directed Mutagenesis

A site-directed mutagenesis technique was performed to generate the $26S^{E738}$ plasmid. This is a PCR-based method to mutate specific nucleotides of a sequence within a plasmid vector (H. Liu & Naismith,

2008). Primers were designed with a partial overlap at the 5' end to avoid self-annealing and the desired base change centered in the overlapping region, p483 and p484 (Table 1). The PCR contained 200 ng/µL of template, 0.5 µM of each primer, 200 µM dNTPs, 0.02 U/µL iProof DNA polymerase, and respective buffer, 5X iProof HF Buffer (Bio-Rad Laboratories). After 5 min at 95°C to denature the template DNA, 25 cycles were initiated, which consisted of 94°C for 30 sec, 55°C for 1 min and 72°C for 10 min (2 min per 1000 bp). The amplified product was then digested with DpnI endonuclease (New England Biolabs) at 37°C for 3 hours to select the mutation-containing synthesized DNA, digesting the parental DNA template.

The mutated plasmid was transformed into chemically competent *E. coli* through heat shock, as previously mentioned. In the next day, individual colonies were isolated and expanded into 5 mL of LB liquid medium with ampicillin antibiotic (100 µg/mL) and incubated overnight at 37°C, with shacking at 200 rpm. Posteriorly, they were extracted using the Zyppy™ Plasmid Miniprep Kit (Zymo Research). After plasmid DNA extraction, concentration and purity were measured using NanoDrop™ 1000 spectrophotometer (Thermo Scientific). Finally, to assess the plasmid correctness, it was sent for sequencing.

## 2.2. Transgene *P. falciparum* cell lines

### 2.2.1. Transfection

After verifying the plasmid identity, it was transfected to a *P. falciparum* Dd2 strain parasite culture. To perform a transfection, it is necessary about 50 µg of plasmid to allow reasonable efficiency. Therefore, *E. coli* containing the plasmid were grown in 300 mL of LB liquid medium, supplemented with ampicillin (100 µg/mL), and incubated overnight at 37°C, with shacking at 200 rpm. Posteriorly, it was extracted using the ZymoPURE™ II Plasmid Maxiprep Kit (Zymo Research), which allows large quantities of a plasmid. Concentration and purity were measured using NanoDrop™ 1000 spectrophotometer (Thermo Scientific).

Transfection was performed by electroporation in uninfected erythrocytes. First, erythrocytes are washed with 5 mL of malaria culture medium (MCM) [RPMI 1640 (Gibco) with 2 mM L-glutamine, 200 µM hypoxanthine, 0.25 µg/mL gentamycin, 25 mM HEPES, 0.2% NaHCO3, and 0.25% Albumax II (Life Technologies)] and then centrifuged at 1500 x*g* for 5 min, to collect them. Next, a second wash was performed with cytomix [10 mM/L $K_2HPO_4/KH_2PO_4$, 120 mM/L KCl, 0.15 mM/L $CaCl_2$, 5 mM/L $MgCl_2$, 25 mM/L HEPES, 2 mM/L EGTA, adjusted with 10 M/L KOH to pH 7.6]. After the wash process, 300

µL of erythrocytes were added to the plasmid solution, which contains 50 µg of plasmid and up to 200 µL of cytomix. This was transferred to a Gene Pulser®/MicroPulserTM Electroporation Cuvettes, 0.2 cm gap (Bio-Rad Laboratories, Inc). The electroporation was performed with 0.31 kV and capacitance of 950 µfD on the Gene Pulser XcellTM (Bio-Rad Laboratories) electroporator. Afterward, the mixture was washed twice in 5 mL of MCM to remove lysed erythrocytes. The transfected erythrocytes were then inoculated with *P. falciparum* Dd2 strain parasite erythrocytes at the trophozoite stage and 5 mL of MCM.

### 2.2.2. *P. falciparum* culture

Parasite cultures were maintained under a controlled atmosphere of 5% $O_2$/5% $CO_2$/90% $N_2$ at 37°C in a $CO_2$ incubator (Thermo Fischer Scientific). Cultures on a t25 flask were maintained at 4% hematocrit in 5 mL of MCM. Medium changes were performed every other day, and cultures' healthiness and parasitemia were regularly monitored by microscopy. This microscopic analysis was performed using a blood smear, fixed with methanol (100%), and colored with 10% Giemsa's azur eosin methylene blue solution (Merck) for 20 min. Parasitemia was calculated by dividing the number of parasitized erythrocytes per total counted erythrocytes.

### 2.2.3. Selection

To select the genetically edited parasites, both cultures were subjected to drug selection. Therefore, first, a selection with WR99210 was performed to select the parasites with the plasmid. After a considerable parasitemia reduction, resistant parasites to WR99210 begin emerging, proceeding to frozen parasites. This process consists of centrifuging the culture at 1500 x*g* for 5 min, to collect the erythrocytes, add the same volume of freezing medium [28% glycerol, 3% sorbitol, and 0.65% NaCl], and store it at -80°C. Posteriorly, a second selection began with neomycin (G418), which allows the selection of parasites with the plasmid integrated since a neomycin cassette present in the pSLI plasmid is only expressed with correct recombination. After a new decrease in the parasitemia, resistant parasites to neomycin appeared, an aliquot was frozen and stored at -80°C, following the procedure mentioned before.

### 2.2.4. Genotyping

After the selection and culture growth, parasites were genotyped and evaluated for the success of genetic manipulation. For that, gDNA was extracted from parasite cultures using the NZY Blood gDNA Isolation kit (NZYTech), as previously described.

To perform the genotyping, a PCR was performed using the forward primer, p39 (Table 1) located in the *P. falciparum* region and the reverse primer, p40 (Table 1) in the *P. chabaudi* region, forming a band of 2370 bp, being posteriorly digested with the restriction enzyme NheI (New England Biolabs). After that, it was sent for sequencing.

## 2.3. Phenotyping

### 2.3.1. Growth Curves

Culture growth was evaluated using a fluorimeter. For that, culture with ring-stage parasites at 0.5% parasitemia and 4% hematocrit was prepared for both lines. To obtain just ring-stage parasites in a culture, it is necessary to synchronize them using sorbitol (5%). During the maturation of the intraerythrocytic stages of the parasite, there is a remodeling of the erythrocytic with *P.* falciparum molecules being exported and incorporated in its plasma membrane. Some of these molecules make the RBC permeable to sorbitol, leading to hypotonic lysis of erythrocytes infected with later-stage parasites, and consequently to its elimination (Maier & Rug, 2012). Thus, cultures are transferred to a tube and centrifuged for 5 min at 1500 x*g* and the supernatant removed. After that, 5 mL of warmed sorbitol (5%) is added and incubated for 15 min at 37°C. Subsequently, it is centrifuged for 5 min at 1500 x*g*, the supernatant withdrawn, and the medium replaced.

Throughout 14 days, 100 µL of culture was retrieved every day to a 96-well plate, and it was stored at -20°C. A blood smear was also performed every day to evaluate the health of the culture since both medium and hematocrit were not changed throughout this time.

To carry out the fluorimeter readings, plates were stained with SYBR green. For this, 4 µM of SYBR green were added to the lysis buffer (15.76 g Tris-HCl, adjust pH to 7.5, 2% w/v EDTA, 0.016% w/v saponin, 1.6% v/v Triton X-100) to a total of 25 µL of the mixture for each well, in a new 96-well plate, where afterward were added 50 µL of the culture in the plates, firstly being necessary to homogenize the culture of each well. Then, after an incubation of 3 hours at RT without light, plates were read in the fluorimeter (Thermo Scientific Varioskan Flash) with excitation and emission wavelength bands at 485 and 530 nm, respectively.

### 2.3.2. Merozoites

Enumeration of merozoites was performed using a blood smear. Firstly, parasites were tightly synchronized using sorbitol (5%) into ring-stage as previously described. Then, after 36 hours, a blood

smear was performed to evaluate the parasite stage. Mature schizonts were observed, and merozoites were counted and normalized per number of schizonts.

### 2.3.3. Half-Maximum Inhibition Concentration ($IC_{50}$)

To perform the drug susceptibility assay, plates were first prepared. In a 96-well microculture plate, 100 µL of MCM were added to the wells, leaving the first column empty. Afterward, 200 µL of DHA previously diluted in MCM to a concentration of 200 µM were added to the first column. The drug must be 2x concentrated once it is diluted by adding 100 µL of parasites. From the first column, 100 µL will be taken and titrated the drug along the columns, discarding the 100 µL after column 10. Columns 11 and 12 were left for control, with no drug added.

After that, tightly synchronized ring-stage parasites at 0.5% parasitemia and 2% hematocrit were added to the plate, 100 µL of the mixture (iRBCs, RBCs, and MCM) to each well. Only RBCs at 2% hematocrit were added for control in the last column. Plates were then incubated for 72 hours at 37°C with a controlled atmosphere (5% $O_2$/5% $CO_2$/90% $N_2$). After the incubation, plates were sealed and frozen at -20°C. Afterward, fluorimeter readings were performed as previously mentioned. $IC_{50}$ values were calculated by nonlinear regression analysis.

### 2.3.4. Ring-Stage Survival Assay (RSA)

To perform the RSA, parasites were synchronized with sorbitol (5%) as previously described, at least 48 hours (1 cycle) before the assay. Afterward, tightly synchronized early ring-stage parasites (0-3h post-invasion), at 0.5% parasitemia and 2% hematocrit, were exposed to 2.5, 5, 10, 20, 50, 250, and 700 nm of DHA. To perform this, plates with the abovementioned concentrations were previously prepared. After 6 hours of incubation at 37°C in the incubator, with a controlled atmosphere (5% $O_2$/5% $CO_2$/90% $N_2$), parasites were centrifuged for 5 min at 1500 x*g*, the supernatant removed and washed three times with phosphate-buffered saline (PBS - 1x). Finally, 1 mL of MCM was added to each pit and incubated for 66 hours. After the incubation time, plates were stored at -20°C. Fluorimeter readings were carried out as previously mentioned. Survival (%) represents the parasitemia normalized to untreated (100%) survival and kill-treated (0% survival) controls, where kill-treated refers to samples treated with 700 nm DHA.

### 2.3.5. Proteasome Activity Analysis

To analyze the proteasome activity, trophozoite-stage parasite cultures at 3% hematocrit and 8% parasitemia were first washed once with PBS (1x) and, consequently, incubated with 0.05% (w/v) saponin for 10 min on ice. Saponin reduces the amount of soluble host cell material in *Plasmodium* spp. Blood-stage preparations. It reacts with cholesterol, forming a complex and changing membrane permeability, leading to host cell lysis (Quadt et al., 2020). Afterward, parasite pellets were washed with ice-cold PBS (1x) three times and lysed at -20°C overnight. It was then cleared by centrifugation at 1000 x*g* for 10 min.

Cell lysates were quantified using the Bradford method, which relies on the binding of the dye Coomassie Brilliant Blue G-250 to the proteins, causing a change in the dye's maximum absorption wavelength from 465 nm to 590 nm, which can be monitored (Kruger, 2003). To perform the quantification, a 96-well plate was used, and 10 µL of the sample was mixed with 200 µL of 1x Bradford's reagent (Bio-Rad Laboratories, Inc). After a 5 min incubation, the absorbances were read at 590 nm. Then, the concentration was determined using a calibration line for bovine serum albumin (BSA) concentration absorbances, which started with a 2000 µg/mL concentration and continued with dilutions of 1:2.

The assay was then performed using the Proteasome Activity Fluorometric Assay Kit II (Ubiquitin-Proteasome Biotechnologies) and following its recommendations. For that, in a 96-well plate, 10 µL of cell lysate were mixed with 20x proteasome assay buffer and 0, 3.125, 6.25, 12.5, and 25 µM of DHA, for a total volume of 50 µL and incubated for 30 min at 37°C. Meanwhile, the proteasome substrate was prepared, mixing 50 µL of 20x proteasome assay buffer with 950 µL $H_2O$, incubating for 10 min at 37°C and, posteriorly, adding 2 µL of 1000x Suc-LLVY-AMC substrate (50 mM in DMSO (dimethyl sulfoxide)) to measure the chymotrypsin-like activity, and stored at 37°C after vortexing for 10 seconds. This substrate is a membrane-permeable fluorogenic substrate consisting of a modified four-mer peptide (succinyl-Leu-Leu-Val-Tyr), conjugated to a 4-amino-7-methylcoumarin (AMC) molecule. The amidation of the AMC molecule extinguishes its fluorescence, which is restored upon recognizing the peptide and cleaving the Tyr-AMC amide bond (Zerfas et al., 2020). After the 30 min incubation, 50 µL of proteasome substrate was added to each pit. Fluorescence was measured at 360/40 nm and 460/30 nm for excitation and emission, respectively, on the spectrophotometer (Thermo Scientific Varioskan Flash), previously heated at 37°C, with readings at every 5 min for 3 hours. For proteasome activity analysis, the slope value of each curve was calculated between 20 and 90 min by using the formula $(Y_{90}-Y_{20})/ (X_{90}-X_{20})$,

in which $Y_{90}$ and $Y_{20}$ were AMC fluorescence readings from the Y-axis at 90 min and 20 min, respectively. Values are normalized to the untreated sample.

### 2.3.6. Levels of ubiquitinated proteins

A Western Blot was performed to evaluate the differences in the levels of ubiquitinated proteins. This technique separates proteins based on their molecular weight through gel electrophoresis. The results obtained from the gel are transferred to a membrane, showing the band for each protein. The proteins are then identified through labeling with the primary antibody and visualized with the help of a secondary antibody (P.-C. Yang & Mahmood, 2012).

For that, trophozoite-stage parasites were first incubated with 5 mL of MCM treated with 0, 0.01, 0.1, 1, 10 µM of DHA for 90 min at 37°C with a controlled atmosphere. Then, trophozoites were isolated using the AutoMacs® Pro Separator (Miltenyi Biotec), separating different stage-parasites using magnetic means. This technique relies upon the fact that *P. falciparum* parasites degrades and feed on hemoglobin when they infect the erythrocyte, generating a toxic iron-containing heme moiety. Parasites avoid its toxicity by transforming it into an inert crystal polymer named hemozoin, which is stored in their food vacuole. The metal in it has an oxidative state different from the one in heme, conferring a paramagnetic property absent in uninfected erythrocytes. The amount of hemozoin increases with the parasite's maturity, bestowing more paramagnetism on the latest stages of *P. falciparum* inside the RBC. Therefore, these latest stages can be separated by passing the culture through a column containing magnetic beads, which become magnetic when placed on a magnetic holder, trapping inside the column the late stage-infected erythrocytes (Coronado et al., 2013). After separation, the eluate was centrifuged at 1500 x*g* for 5 min and washed 3 times with PBS 1x, forming a dark pellet with the parasites. The supernatant was discarded, and 50 µL of $H_2O$ was added, storing at -20°C to lyse the parasites. Afterward, lysates were cleared by centrifugation for 15 min at 5000 x*g* at 4°C and supernatant was collected. Protein quantification was assessed using the Bradford method previously described.

Electrophoresis was performed using a running gel of 12% sodium dodecyl sulfate-polyacrylamide gel electrophoresis (SDS-PAGE) and a stacking gel of 5% SDS-PAGE. Protein samples were prepared by adding 20 µg of total protein to 10 µL of loading buffer, previously prepared by adding 50 µL of 2-mercaptoethanol to 950 µL of 2x Laemmli Sample Buffer (Bio-Rad Laboratories). A denaturation step at 98°C for 5 min was performed next. The samples were loaded onto the gel and separated by

electrophoresis (100V). Gels were then transferred to a nitrocellulose membrane (Bio-Rad Laboratories) in Trans-Blot Turbo Transfer Buffer (Bio-Rad Laboratories) using the Trans-Blot Turbo Transfer System (Bio-Rad Laboratories). To prevent unspecific connections, the membranes were blocked with 5% of BSA in Tris-Buffered Saline (TBS)/0,1% Tween 20 for 1h at RT and then incubated overnight with the primary antibodies at 4°C (Table 2). Actin was used as the loading control. On the next day, the membranes were washed in TBS/0,1% tween three times, each of 5 min, and then incubated with a fluorescent secondary antibody for 1 hour (Table 3). Sapphire Biomolecular Imager (Azure Biosystems) was used for protein detection. Quantitative analyses were performed using the ImageJ software.

**Table 2. List of primary antibodies used on the Western Blot and respective information.**

| Protein Target | Dilution | Source | Brand |
|---|---|---|---|
| Ubiquitin | 1:1000 | Rabbit | Invitrogen |
| Actin | 1:1000 | Mouse | Invitrogen |

**Table 3. List of secondary antibodies used on the Western Blot and respective information.**

| Antiserum | Dilution | Host | Conjugate | Brand |
|---|---|---|---|---|
| Anti-Rabbit | 1:1000 | Goat | DyLight 488 | Invitrogen |
| Anti-Mouse | 1:1000 | Goat | DyLight 680 | Invitrogen |

### 2.3.7. Statistical Analysis

Statistical analysis was performed using the GraphPad Prism 8 software. Results were presented as means ± standard error of the mean (SEM). Comparisons between different conditions were performed using *t*-tests and two-way ANOVA. Differences were considered significant in the statistical analysis when $p<0.05$. At least three biological replicates were performed for each assay.

# 3. Results and Discussion

Malaria remains one of the leading causes of mortality worldwide, especially in tropical regions. Of all *Plasmodium* species capable of infecting humans, *P. falciparum* is the most virulent, due to its ability of cytoadherence, obstructing perfusion and, therefore, evading immune system clearance, being responsible for the majority of deaths and, thus, the main focus of this dissertation (Josling & Llinás, 2015).

ACTs are currently the most used antimalarial, which has helped reduce the malaria incidence observed in the last years. However, this treatment demonstrates an increased parasite clearance time, highlighting an ACT resistance problem. This might be due to parasites developing mechanisms to cope with short but powerful peaks of ART drug exposure due to his short half-life. This resistance to ART and the partner drug is still very localized, being of extreme importance to understand the mechanisms behind it, to prevent its spread and the increase of malaria burden.

## 3.1. Plasmid construction

A partner group laboratory investigated the genome of ACT-resistant *P. chabaudi* parasites to find associated mutations. As a result, a SNV in the 26S proteasome regulatory subunit *rpn2* gene was found thought to alter their protein's network interactions. Since other mutations were found on these parasite lines, there was the need for isolation of this mutation to evaluate its contribution to resistance to artemisinin. Additionally, *in vitro*, *P. chabaudi* parasites rupture during schizogony (asexual maturation) turning unsuitable for laboratorial handling (Marr et al., 2020; Spence et al., 2011).

Therefore, to evaluate the impact of this SNV in the proteasome function and the artemisinin response in *P. falciparum*, a plasmid was constructed to design a functional chimeric gene with parts of the gene from *P. falciparum* and the part from *P.* chabaudi. Protein sequence alignment shows 78.6% identity between the *rpn2* gene from the *P. chabaudi* and from the *P. falciparum* (Figure 6A). The E738K variant was studied after generating the $26S^{E738}$ and $26S^{738K}$ plasmids, as shown in the strategy scheme (Figure 6B).

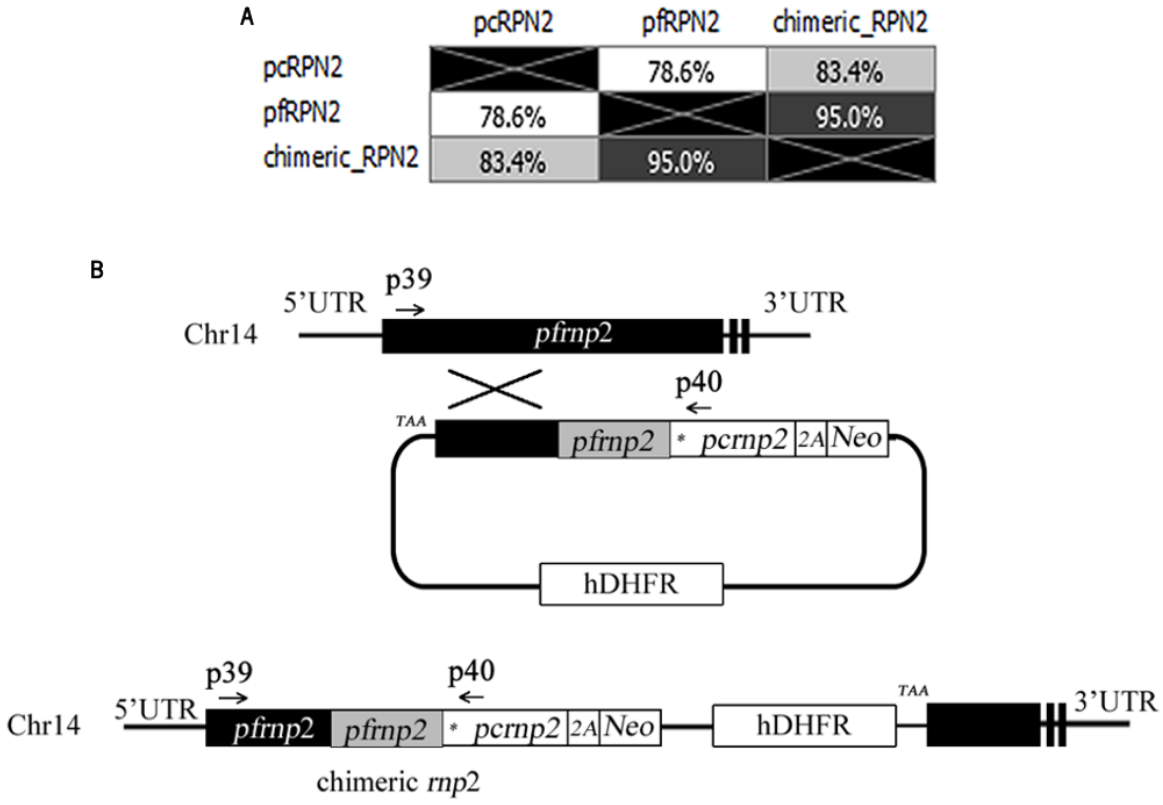


**Figure 6. Strategy and plasmid construction for 738K variant. A.** Identity matrix of the results from the protein sequence BLOSUM95 alignment between *P. chabaudi*, *P. falciparum*, and the chimeric rpn2 hybrid. **B.** Strategy to construct a plasmid with the 738K variant. Using the Selection-Linked Integration (SLI) technique, a plasmid with part of the *P. falciparum rpn2* gene and part of the *P. chabaudi rpn2* gene, where the E738K is located (marked with an asterisk). Primers p39 and p40 (Table 1) were used to identify plasmid genomic integration by PCR.

This plasmid was constructed using the Selection-linked Integration (SLI) technique. In this approach, a region homologous to the target locus, the *P. falciparum* part, is necessary to promote a single crossover integration of the plasmid, followed by the gene of interest. This is linked to an additional selectable marker, in this case, the neomycin resistance cassette, being separated by a skip peptide (T2A), which does not allow the attachment to the target itself. Since the resistance marker does not have a promoter, it will only confer resistance if the integration occurs at the desired recombination locus, expressed through the endogenous gene's promoter (Birnbaum et al., 2017). This integration of the selectivity marker together with the gene of interest only works due to T2A (family of 2A self-cleaving peptides), once formed after the translation process in protein synthesis, gives rise to a protein chemically fragile that self cleaves, promoting the separation of the protein of interest from the protein formed by the translation of the selection marker protein, preventing the formation of a dysfunctional protein (protein

from the selectivity marker coupled to the protein of interest) (Z. Liu et al., 2017). This technique in addition to neomycin, which is promoterless, it presents an additional resistance marker with a promoter, *hDHFR* (human dihydrofolate reductase), conferring resistance to WR99210 and allowing the initial selection of parasites that contain the episomal SLI plasmid (Birnbaum et al., 2017). This method made it possible to obtain cell lines with genomic integrations in *P. falciparum* with a greater speed and success rate.

A descendent plasmid was then constructed with the E738 variant using the site-directed mutagenesis technique to replace a lysine for a glutamic acid on the 738 position. As mentioned before, this is a PCR-based method used to introduce DNA modifications within a plasmid vector. In this technique, primers are designed with a partial overlap at the 5' end to avoid self-annealing and the desired base change centered in the overlapping region (H. Liu & Naismith, 2008). The amplified product is digested with DpnI endonuclease to select the mutation-containing synthesized DNA, digesting the parental DNA template and reducing the number of nonmutagenized colonies after transformation (J. Li et al., 2008; H. Liu & Naismith, 2008).

## 3.2. *P. falciparum* transfection

Both plasmids, with the E738 and the 738K variant, were then transfected into Dd2 *P. falciparum* parasites cell lines, a multi-drug resistant strain derived from an Indochina isolate (Reilly et al., 2007). Plasmids transfection were performed by electroporation into unparasitized RBCs and posteriorly mixed with trophozoite-stage parasitized RBCs. This process avoids the death of parasites induced by the electric shock into infected parasites (Hasenkamp et al., 2012). Parasites were posteriorly subjected to WR99210 to select the transfected parasites with episomal SLI plasmid (pSLI). After a decrease in the parasitemia and a return to a parasitemia of 2%, it was exposed to neomycin to select parasites with the plasmid genome integrated since a promoterless resistance cassette is present, as mentioned before (Figure 7A).

After the selection and to assess the correctness of the transfected cultures, a PCR was performed using the forward primer located in the *P. falciparum* region and the reverse primer in the *P. chabaudi* region, forming a band of 2370 bp. Due to the location of the primers, it was not expected to appear a band in the parental line (Dd2 WT). Afterward, digestion with NheI was performed, being expected to have a band near 2000 bp and another with approximately 300 bp (Figure 7B). The PCR product was sent for sequencing to confirm the different variants (Figure 7C). In the sequencing electropherogram, it is possible to observe that the E738 variant is present in the *rpn2* gene sequence of *P. chabaudi* (PCHAS_133430), and no restriction site for the NheI enzyme is present. On the other hand,

in the mutated parasite lines, a restriction site for NheI is observed, as well as both variants, E738, and 738K, in the different lines, confirming the successful genetic engineering of the parasite lines.

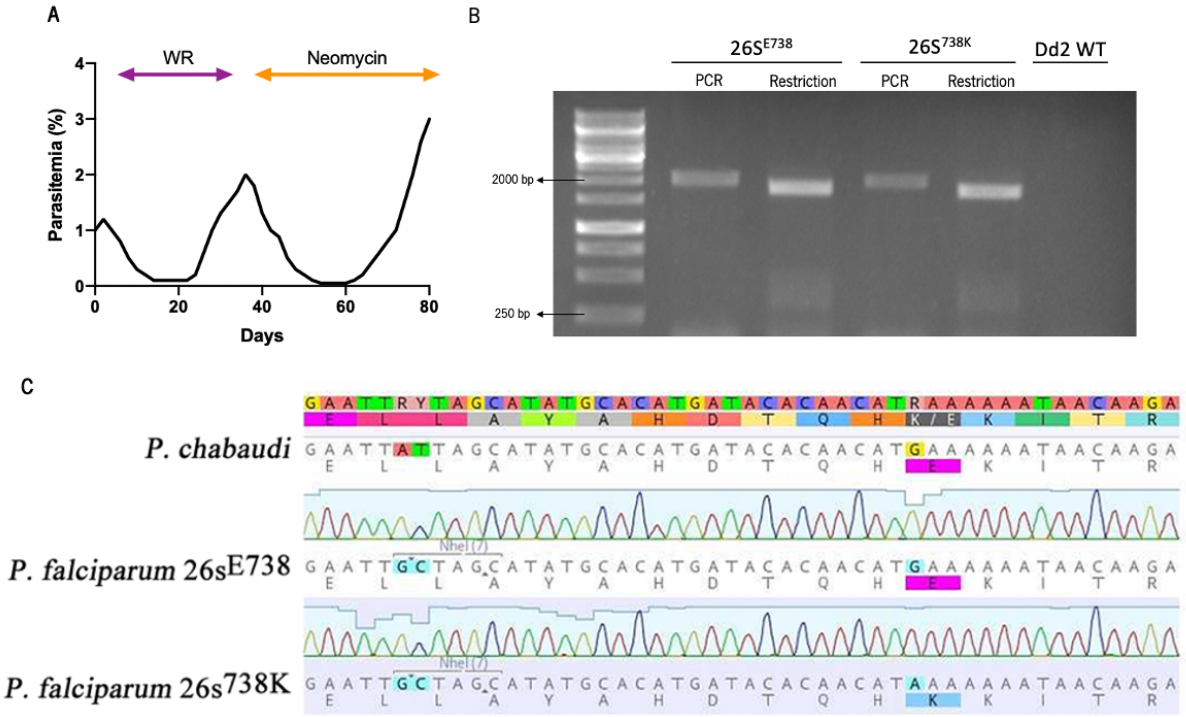


**Figure 7. Analysis of the transfection efficacy. A.** Representative growth graph of transfected cultures under selection with WR99210 and Neomycin. **B.** PCR detection of plasmid genomic integration for Dd2 $26S^{E738}$ and Dd2 $26S^{738K}$. PCR restriction with NheI was used to map the fragment. **C.** PCR sequencing for confirmation of synonymous mutation engineering for the NheI restriction site and non-synonymous E738K variants parasite lines.

## 3.3. Parasite Growth Analysis

A different growth pattern was observed during the maintenance of the two cultures with the variants. To understand these differences, the growth was analyzed with the parasitemia count every day for 14 days. With this experiment, it was possible to observe that the 738K variant had slower culture growth than the E738 variant (Figure 8A). To understand if the growth difference was due to metabolic differences or cellular multiplication alteration, the number of merozoites was counted on both parasite lines. It was observed that $26S^{E738}$ parasites presented a greater number of merozoites per schizont, an average of 14, compared to $26S^{738K}$ parasites, an average of approximately 12. However, this difference was not statistically significant (Figure 8B). In the Dd2 strain, between 8 and 28 merozoites are usually counted, with an average of 18 merozoites per schizont (Simon et al., 2021). Therefore,

although the count was within the merozoite range counted usually in the Dd2 strain, the average was lower in both parasite lines.

At the end of schizogony, cytokinesis results in the development of new merozoites, which are then released by rupture of the host erythrocyte. During schizogony, cellular structures as secretory organelles, rhoptries, and dense granules are elaborated. Parasites also modify their host cell, secreting several proteins into the cytoplasm and affecting the erythrocyte's cytoskeleton and surface. Merozoite's secretory organelles are dismantled after the invasion, increasing protein ubiquitylation. Therefore, protein degradation processes are essential for the asexual intraerythrocytic cycle. In addition, inhibition of the UPS results in the reduction of parasite infection (Green et al., 2020; Rashidi et al., 2021). Accordingly, 738K variant may have an influence on the proteasome function in the schizogony stage, resulting in slower growth and having difficulty in reaching high parasitemia's.

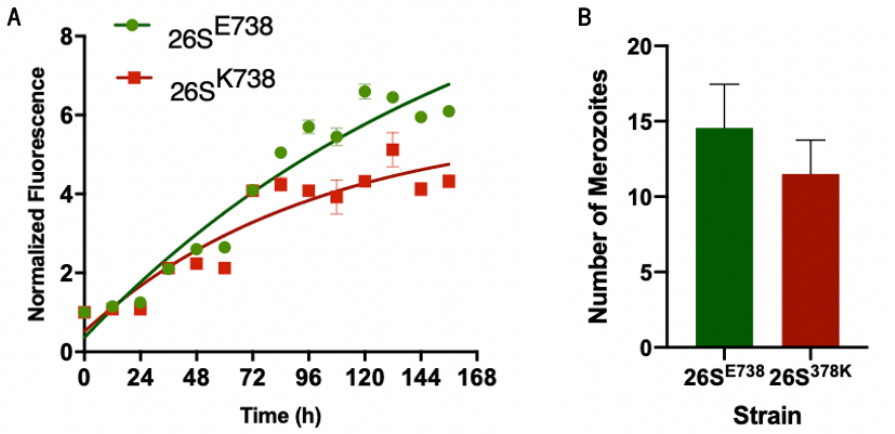


**Figure 8. 26S$^{738K}$ presents decreased growth in comparison with 26S$^{E378}$. A.** Growth curves of parasite lines 26S$^{E738}$ and 26S$^{738K}$. Parasitemia was evaluated every day for 14 days. **B.** Mean ± SEM of merozoites number within schizonts are represented for parasite lines 26S$^{E738}$ and 26S$^{738K}$.

## 3.4. Susceptibility assays

### 3.4.1. Half maximal inhibitory concentration ($IC_{50}$)

To assess the impact of the E378K variant on the DHA response, drug susceptibility assays were performed. The number of alive parasites previously exposed to serial dilutions of DHA was quantified through fluorimeter readings, and the $IC_{50}$ was calculated. The 738K variant leads to a significant

increase in the $IC_{50}$ compared to the E738 variant (Figure 9A and 9B), with values of 2.25 nM and 0.8 nM, respectively.

Typically, the $IC_{50}$ values for DHA vary between 0 and 8 nM in *P. falciparum* (Fairhurst & Dondorp, 2016). Therefore, both parasite lines are within the strain $IC_{50}$ interval. However, since there is a significant difference, that might indicate a difference regarding artemisinin response. Nevertheless, *in vivo* parasite clearance half-lives correlate poorly with DHA 50% inhibitory concentrations *in vitro*, being necessary other drug susceptibility assays to evaluate the difference in the artemisinin response in parasites bearing the 738K variant (Fairhurst & Dondorp, 2016).

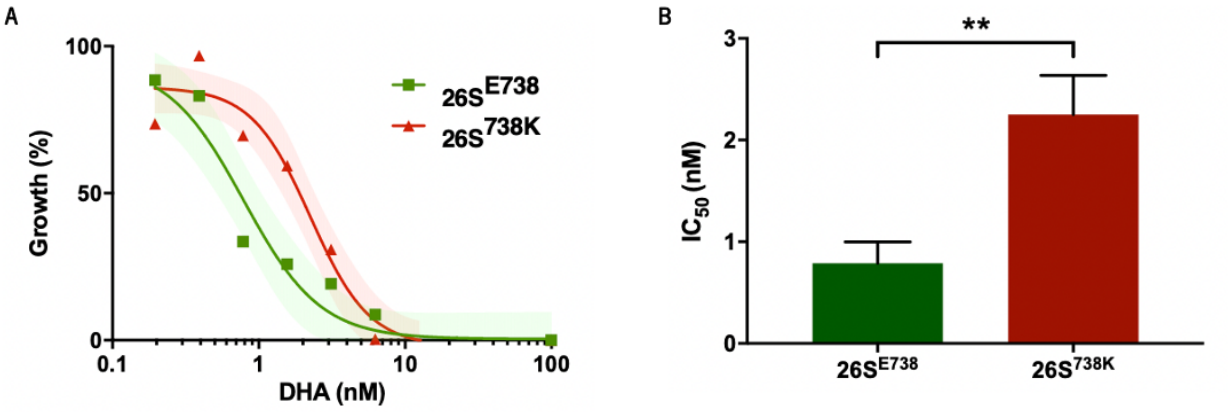


**Figure 9. 738K variant increases IC50 to DHA.** In vitro $IC_{50}$ of $26S^{E738}$ and $26S^{738K}$. Ring-Stage parasites were exposed to a range of DHA concentrations for 72 hours. **A.** Dose-response curves are plotted from mean % inhibition ± SEM. **B.** Mean ± SEM $IC_{50}$ values are represented for dihydroartemisinin. Three assays were performed for each line. Statistical evaluations comparing both lines were performed using unpaired *t*-tests. $^{**}p<0.01$

### 3.4.2. Ring-Stage Survival Assay (RSA)

Artemisinin resistance was difficult to study in the beginning due to poor correlation with the standard *in vitro* measures of susceptibility, which complicated the initial research into slow-clearing *P. falciparum* in Cambodia (Dondorp et al., 2009; Noedl et al., 2008). It was posteriorly discovered that parasite resistance to ARTs did not emerge across the whole parasite life cycle, and it was only identifiable in the ring stage of development (Khoury et al., 2020). Given the need for a more reliable and standardized *in vitro* measure of delayed clearance that correlates with the *in vivo* resistance phenotype, the ring-stage

survival assay (RSA) was developed (Witkowski et al., 2013). This method consists of tightly synchronizing cultured parasites at the early ring stage (2-4 hours post-invasion) and subjecting them to a 6-hour pulse of DHA. After 72 hours, the parasite survival rate is evaluated (Sutherland et al., 2020; J. Zhang et al., 2017).

Therefore, a RSA was performed to confirm the impact on the response to artemisinin. It was possible to observe a significant difference at 2.5, 5, and 10 nM of DHA between both lines, with the 738K variant demonstrating increased parasite survival (Figure 10A). The assay was also performed in trophozoites. However, although $26S^{738K}$ parasites present higher parasite survival, there was no significant difference between both lines at trophozoite stages (Figure 10B). This difference between the assay in rings and trophozoites demonstrates that later parasite stages are highly susceptible to ART, unlike early ring-stage parasites that are able to survive pulses of DHA (Davis et al., 2020). This profile coincides with the peal period of hemoglobin uptake and degradation, during which $Fe^{2+}$-heme is liberated and activated ART (Stokes et al., 2019).

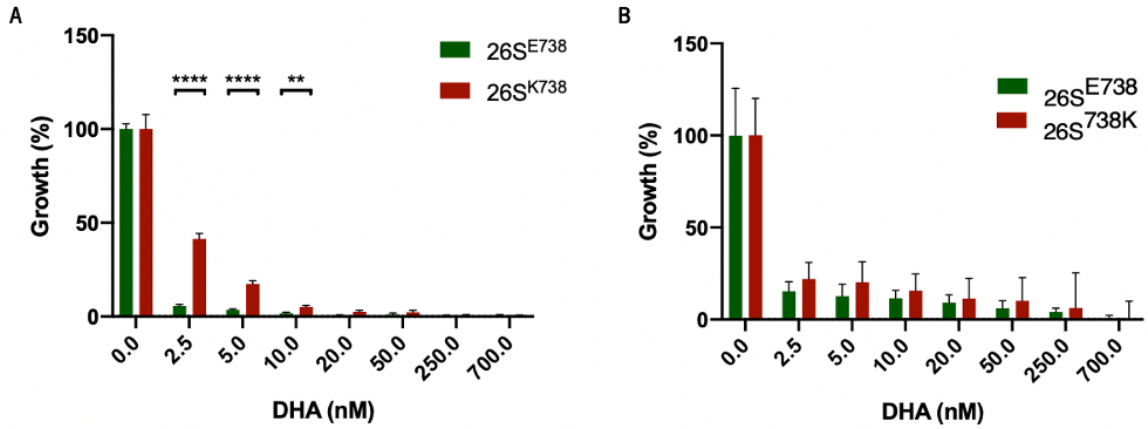


**Figure 10. 738K variant influences susceptibility to DHA. A.** Young rings (0-3h post-invasion) of the $26S^{E738}$ and $26S^{738K}$ lines were treated with DHA pulse for 6h. RSA survival rate ± SEM) was measured. **B.** Trophozoite-stage parasites of the $26S^{E738}$ and $26S^{738K}$ were subjected to the treatment mentioned above, and survival rates ± SEM were measured. Three assays were performed for each line. Statistical evaluations comparing lines were performed using *t*-tests. $^{**}p<0.01$, $^{****}p<0.0001$.

## 3.5. Proteasome activity

DHA reacts with susceptible groups in biomolecules in its activated state, causing cellular damage. These damaged proteins are marked posteriorly with ubiquitin, rapidly increasing the accumulation of ubiquitinated proteins in DHA-treated parasites. This rapid accumulation may clog the proteasome and lead to the inhibition of its activity (Bridgford et al., 2018).

Taking this into account, the chymotrypsin-like activity of the proteasome was analyzed. In this essay, the proteasome cleaves the Suc-LLVY-AMC substrate, a fluorogenic substrate, while the released AMC fluorescence is monitored. It was possible to observe that proteasome activity decreases when DHA is added in all lines, continuing to decline with increasing drug concentration. However, parasites with the 738K variant presented a smaller proteasome activity decline than both parental and $26S^{E738}$ parasite lines in all concentrations. In fact, it was observed a significantly higher proteasome activity compared with the other lines, increasing the difference in the highest concentrations, at 12.5 μM and 25 μM in $26S^{E738}$ parasite lines and 25 μM in the parental line (Dd2 WT) (Figure 11A).

Since the proteasome activity is inhibited with DHA in WT parasites (Bridgford et al., 2018), the accumulation of polyubiquitinated proteins may increase, causing oxidative stress and inducing parasite death. However, since $26S^{738K}$ parasites present higher proteasome activity, this accumulation should be smaller. Therefore, a western blot was performed to assess if there were increased polyubiquitinated proteins in DHA-treated parasites and compare the $26S^{738K}$ parasites accumulation with the other lines (Figure 11B).

For the western blot, trophozoite-stage parasites of all lines were submitted to different concentrations of DHA for 90 min, lysed with saponin, and posteriorly the protein extracted. In its analysis, it was possible to observe an accumulation of polyubiquitinated proteins in the parental line and the $26S^{E738}$ parasites line compared with the baseline (without DHA). However, in the $26S^{738K}$ parasites line, the relative ubiquitin expression, considering actin expression, presented a slight decrease throughout the concentrations, being significantly smaller compared to the other lines at 10 μM of DHA (Figure 11C).

It was shown that, in addition to causing cellular damage, DHA also disrupts proteasome-dependent degradation, preventing damaged proteins removal. This last one was observed with the

accumulation of polyubiquitinated proteins. This is a double threat to the parasite and further induces oxidative stress, leading to the death of the parasites. Nevertheless, it was also shown that parasites with the 738K variant have less inhibition of the proteasome activity, as well as a consequent decrease on the accumulation of polyubiquitinated proteins. This suggests that this variant antagonizes the physiological impact of DHA controlled by the 26S proteasome.

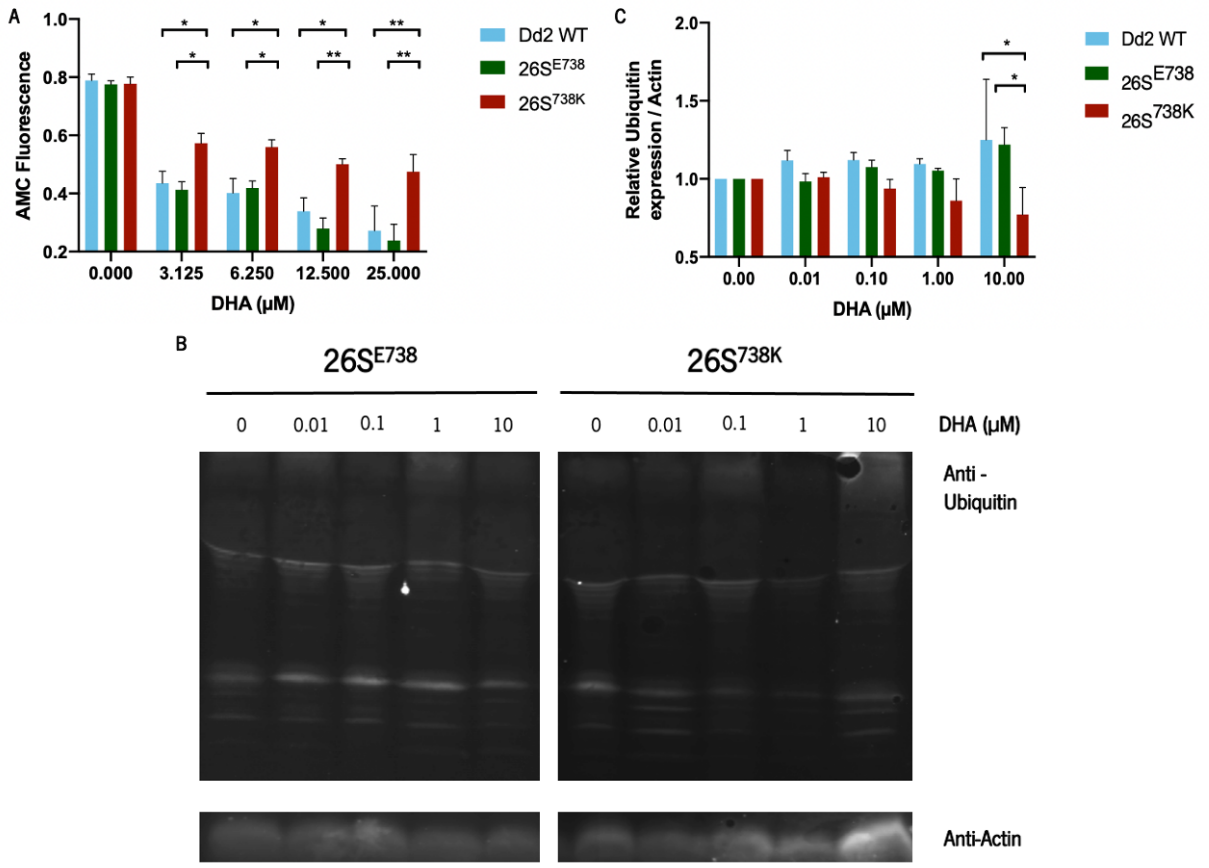


**Figure 11. 26S$^{738K}$ parasites have increased proteasome activity. A.** Trophozoite-stage parasites of the Dd2 WT, 26S$^{E738}$, and 26S$^{738K}$ lines, were incubated with DHA for 30 min. The chymotrypsin-like activity was measured using the fluorogenic substrate Suc-LLVY-AMC for 3 hours. Slope value ± SEM was calculated using readings between 20- and 90-min. **B.** Representative western blot. Trophozoite-stage parasites of the Dd2 WT, 26S$^{E738}$, and 26S$^{738K}$ lines, were incubated with DHA for 90 min, and protein was subsequently extracted to analyze protein polyubiquitination. **C.** Western Blot analysis. Relative ubiquitin expression considering actin expression. Ubiquitin values were normalized to the baseline (without DHA). Three assays were performed for each line in both essays. Statistical evaluations comparing lines were performed using a two-way ANOVA. *$p$<0.05, **$p$<0.01.

This mutation is present in the rpn2 subunit, which serves as a scaffold to ubiquitin-processing factors and is involved in stabilizing the 19S RP, responsible for the recognition of ubiquitylated substrates (Kors et al., 2019; Mao, 2021). A study in the human proteasome demonstrated that kinase p38 MAPK (Mitogen-Activated Protein Kinase) phosphorylated the rpn2 subunit, being Thr-273 of rpn2 the major phosphorylation site affected, stabilizing the poly- and non-ubiquitinated substrates and reducing all three proteolytic activities of the proteasome, caspase-, trypsin- and chymotrypsin-like activities. Additionally, this study also demonstrated that a T273A mutation in the rpn2 blocked the p38 MAPK-mediated proteasome inhibition. Other studies demonstrated that rpn2 interacts with rpt3, rpt4, and rpt6 of the proteasome ATPase complex, which are involved in regulating the 20S CP gate opening (Lee et al., 2010). This suggests that alteration in rpn2 protein has major impact downstream of the 26S proteasome mediated protein degradation process.

# 4. Conclusion

Despite decades of clinical research and treatment procedures, malaria is a global disease burden, being *P. falciparum* the primary species responsible for it. As the utilization and effectiveness of experimental vaccines have been minimal, there is a significant reliance on antimalarial drugs for prophylaxis and treatment of infected patients. Consequently, antimalarials are among the most widely used drugs in tropical areas. The high demand for treatment, worsened to some extent by incomplete patient adherence, exerts enormous drug selection pressure on *P. falciparum* parasites to evolve resistance mechanisms (Wicht et al., 2020).

Artemisinin and its derivatives rapidly reduce the parasite burden in *P. falciparum* infection. For this reason, nowadays, antimalarial control is highly dependent on ACTs, the combination of an ART with a longer-lasting partner drug. Moreover, decreased sensitivity to ARTs is emerging, making it critical to understand the mechanism of action of ARTs and their resistance (Bridgford et al., 2018).

The ubiquitin-proteasome system is a large and very complex proteomic network system. It is one of the main pathways responsible for regulating protein abundance levels and protein activities. Protein turnover, transcriptional regulation, cell cycle progression, differentiation, and signal transduction are some of the biological activities it plays a role (Hamilton et al., 2014). Additionally, it may also be involved in the mechanism of action of ARTs since they cause damage in parasite biomolecules, causing cellular damage and oxidative stress (Blasco et al., 2017). The finding of several mutations in several associated genes suggests that the evolution and spread of linked resistance to artemisinin may occur in different manners. From a public health point of view, this raises concerns since geographically genetic markers can differ.

The E738K is a SNV found in ACTs resistant parasites from the *P. chabaudi* species in the rpn2 subunit of the 26S proteasome. In the protein sequence alignment between *P. falciparum* and *P. chabaudi* rpn2 subunit, there is a 78.6% of homology. Therefore, to study the E738K variant, two plasmids were manufactured with part of the *P. falciparum* gene and part of the *P. chabaudi*, where the variant is located. Afterward, both plasmids were transfected into Dd2 *P. falciparum* parasites, creating the $26S^{E738}$ and the $26S^{738K}$ parasite lines.

In the assays performed in these parasite lines, it was possible to observe a different growth pattern, as well as different merozoites count, where the $26S^{738K}$ parasites present a slower growth. Additionally, this parasite line presented increased $IC_{50}$ values and significant differences in the parasite survival in the RSA. Regarding the proteasome activity, parasites bearing the 738K present increased

chymotrypsin-like activity when subjected to DHA and decreased accumulation of polyubiquitinated proteins.

Altogether, these results suggest that the 738K variant confer DHA resistance to the parasites since there is increased parasite survival when subjected to DHA. Furthermore, considering the proteasome activity assay and the polyubiquitinated proteins assay, it suggests that the proteasome has an important role in this DHA resistance. Moreover, it demonstrates that the ubiquitin-proteasome pathway plays an important role in the DHA mechanism of action since an increased proteasome activity in parasites with DHA increases the parasite survival.

Therefore, other mutations in this subunit of the proteasome may have an impact on the proteasome activity by modifying downstream steps of the degradation process. One hypothesis to understand the impact of the 738K variant in proteasome activity may be that DHA phosphorylates the glutamic acid present in the 738 position, which may be necessary to trigger proteasome inhibition. When the amino acid is changed to lysine in this position, similar to the T234A mutation, it prevented proteasome inhibition. Accordingly, the amount of polyubiquitinated proteins does not increase until the reaching point of oxidative stress and, consequently, parasite death.

Overall, this dissertation provides progression in understanding the proteasome's role in the DHA mechanism of action and parasite response to it. Our data supports the hypothesis that DHA might interact directly with the 26S proteasome in *P. falciparum*, being the first report of a mutation in a DHA drug target, rising resistance. Nevertheless, in the future, it is essential to understand how this change of an amino acid in the E738K variant has impacted the proteasome activity, proving whether DHA phosphorylates glutamic acid in this position or if it is through other posttranslational modification. Furthermore, it is important to understand how it impacts the growth of the parasites, as well as the number of merozoites per schizont.

# 5. Bibliography


Aminake, M. N., Arndt, H.-D., & Pradel, G. (2012). The proteasome of malaria parasites: A multi-stage drug target for chemotherapeutic intervention? *International Journal for Parasitology: Drugs and Drug Resistance*, *2*, 1–10.

Antony, H., & Parija, S. (2016). Antimalarial drug resistance: An overview. *Tropical Parasitology*, *6*(1), 30.

Ashley, E. A., Dhorda, M., Fairhurst, R. M., Amaratunga, C., Lim, P., Suon, S., Sreng, S., Anderson, J. M., Mao, S., Sam, B., Sopha, C., Chuor, C. M., Nguon, C., Sovannaroth, S., Pukrittayakamee, S., Jittamala, P., Chotivanich, K., Chutasmit, K., Suchatsoonthorn, C., … White, N. J. (2014). Spread of Artemisinin Resistance in *Plasmodium falciparum* Malaria. *New England Journal of Medicine*, *371*(5), 411–423.

Ashley, E. A., & Phyo, A. P. (2018). Drugs in Development for Malaria. *Drugs*, *78*(9), 861–879.

Ashley, E. A., Pyae Phyo, A., & Woodrow, C. J. (2018). Malaria. *The Lancet*, *391*(10130), 1608–1621.

Belachew, E. B. (2018). Immune Response and Evasion Mechanisms of *Plasmodium falciparum* Parasites. *Journal of Immunology Research*, *2018*, 1–6.

Birnbaum, J., Flemming, S., Reichard, N., Soares, A. B., Mesén-Ramírez, P., Jonscher, E., Bergmann, B., & Spielmann, T. (2017). A genetic system to study *Plasmodium falciparum* protein function. *Nature Methods*, *14*(4), 450–456.

Blasco, B., Leroy, Di., & Fidock, D. A. (2017). Antimalarial drug resistance: linking *Plasmodium falciparum* parasite biology to the clinic. *Nature Medicine*, *23*(8), 917–928.

Bozdech, Z., Ferreira, P. E., & Mok, S. (2015). A crucial piece in the puzzle of the artemisinin resistance mechanism in *Plasmodium falciparum*. *Trends in Parasitology*, *31*(8), 345–346.

Bridgford, J. L., Xie, S. C., Cobbold, S. A., Pasaje, C. F. A., Herrmann, S., Yang, T., Gillett, D. L., Dick, L. R., Ralph, S. A., Dogovski, C., Spillman, N. J., & Tilley, L. (2018). Artemisinin kills malaria parasites by damaging proteins and inhibiting the proteasome. *Nature Communications*, *9*(1), 1–9.

Coppée, R., Jeffares, D. C., Miteva, M. A., Sabbagh, A., & Clain, J. (2019). Comparative structural and evolutionary analyses predict functional sites in the artemisinin resistance malaria protein K13. *Scientific Reports*, *9*(1), 10675.

Coronado, L. M., Tayler, N. M., Correa, R., Giovani, R. M., & Spadafora, C. (2013). Separation of *Plasmodium falciparum* Late Stage-infected Erythrocytes by Magnetic Means. *Journal of Visualized Experiments*, *73*.

Cowman, A. F., Healer, J., Marapana, D., & Marsh, K. (2016). Malaria: Biology and Disease. *Cell*, *167*(3), 610–624.

Davis, S. Z., Singh, P. P., Vendrely, K. M., Shoue, D. A., Checkley, L. A., McDew-White, M., Button-Simons, K. A., Cassady, Z., Sievert, M. A. C., Foster, G. J., Nosten, F. H., Anderson, T. J. C., & Ferdig, M. T. (2020). The extended recovery ring-stage survival assay provides a superior association with patient clearance half-life and increases throughput. *Malaria Journal*, *19*(1), 54.

Digaleh, H., Kiaei, M., & Khodagholi, F. (2013). Nrf2 and Nrf1 signaling and ER stress crosstalk: implication for proteasome degradation and autophagy. *Cellular and Molecular Life Sciences*, *70*(24), 4681–4694.

Dogovski, C., Xie, S. C., Burgio, G., Bridgford, J., Mok, S., McCaw, J. M., Chotivanich, K., Kenny, S., Gnädig, N., Straimer, J., Bozdech, Z., Fidock, D. A., Simpson, J. A., Dondorp, A. M., Foote, S., Klonis, N., & Tilley, L. (2015). Targeting the Cell Stress Response of *Plasmodium falciparum* to Overcome Artemisinin Resistance. *PLOS Biology*, *13*(4), e1002132.

Dondorp, A. M., Nosten, F., Yi, P., Das, D., Phyo, A. P., Tarning, J., Lwin, K. M., Ariey, F., Hanpithakpong, W., Lee, S. J., Ringwald, P., Silamut, K., Imwong, M., Chotivanich, K., Lim, P., Herdman, T., An, S. S., Yeung, S., Singhasivanon, P., … White, N. J. (2009). Artemisinin Resistance in *Plasmodium falciparum* Malaria. *New England Journal of Medicine*, *361*(5), 455–467.

Douine, M., Lazrek, Y., Blanchet, D., Pelleau, S., Chanlin, R., Corlin, F., Hureau, L., Volney, B., Hiwat, H., Vreden, S., Djossou, F., Demar, M., Nacher, M., & Musset, L. (2018). Predictors of antimalarial self-medication in illegal gold miners in French Guiana: a pathway towards artemisinin resistance. *Journal of Antimicrobial Chemotherapy*, *73*(1), 231–239.

Eastman, R. T., & Fidock, D. A. (2009). Artemisinin-based combination therapies: a vital tool in efforts to eliminate malaria. *Nature Reviews Microbiology*, *7*(12), 864–874.

Fairhurst, R. M., & Dondorp, A. M. (2016). Artemisinin-Resistant *Plasmodium falciparum* Malaria. In *Emerging infections 10* (pp. 409–429). American Society of Microbiology.

Ferreira, P. E., Culleton, R., Gil, J. P., & Meshnick, S. R. (2013). Artemisinin resistance in *Plasmodium falciparum*: what is it really? *Trends in Parasitology*, *29*(7), 318–320.

Green, J. L., Wu, Y., Encheva, V., Lasonder, E., Prommaban, A., Kunzelmann, S., Christodoulou, E., Grainger, M., Truongvan, N., Bothe, S., Sharma, V., Song, W., Pinzuti, I., Uthaipibull, C., Srichairatanakool, S., Birault, V., Langsley, G., Schindelin, H., Stieglitz, B., … Holder, A. A. (2020). Ubiquitin activation is essential for schizont maturation in *Plasmodium falciparum* blood-stage development. *PLOS Pathogens*, *16*(6), e1008640.

Hamilton, M. J., Lee, M., & Le Roch, K. G. (2014). The ubiquitin system: an essential component to unlocking the secrets of malaria parasite biology. *Mol. BioSyst.*, *10*(4), 715–723.

Hasenkamp, S., Russell, K. T., & Horrocks, P. (2012). Comparison of the absolute and relative efficiencies of electroporation-based transfection protocols for *Plasmodium falciparum*. *Malaria Journal*, *11*(1), 210.

Hunt, P., Afonso, A., Creasey, A., Culleton, R., Sidhu, A. B. S., Logan, J., Valderramos, S. G., McNae, I., Cheesman, S., Rosario, V. do, Carter, R., Fidock, D. A., & Cravo, P. (2007). Gene encoding a deubiquitinating enzyme is mutated in artesunate- and chloroquine-resistant rodent malaria parasites. *Molecular Microbiology*, *65*(1), 27–40.

Josling, G. A., & Llinás, M. (2015). Sexual development in *Plasmodium* parasites: knowing when it's time to commit. *Nature Reviews Microbiology*, *13*(9), 573–587.

Khoury, D. S., Cao, P., Zaloumis, S. G., & Davenport, M. P. (2020). Artemisinin Resistance and the Unique Selection Pressure of a Short-acting Antimalarial. *Trends in Parasitology*, *36*(11), 884–887.

Kors, S., Geijtenbeek, K., Reits, E., & Schipper-Krom, S. (2019). Regulation of Proteasome Activity by (Post-)transcriptional Mechanisms. *Frontiers in Molecular Biosciences*, *6*.

Krishnan, K. M., & Williamson, K. C. (2018). The proteasome as a target to combat malaria: hits and misses. *Translational Research*, *198*, 40–47.

Kruger, N. J. (2003). The Bradford Method for Protein Quantitation. In *Basic Protein and Peptide Protocols* (Vol. 32, pp. 9–16). Humana Press.

Lee, S.-H., Park, Y., Yoon, S. K., & Yoon, J.-B. (2010). Osmotic Stress Inhibits Proteasome by p38 MAPK-dependent Phosphorylation. *Journal of Biological Chemistry*, *285*(53), 41280–41289.

Li, H., Bogyo, M., & da Fonseca, P. C. A. (2016). The cryo-EM structure of the *Plasmodium falciparum* 20S proteasome and its use in the fight against malaria. *The FEBS Journal*, *283*(23), 4238–4243.

Li, J., Li, C., Xiao, W., Yuan, D., Wan, G., & Ma, L. (2008). Site-directed mutagenesis by combination of homologous recombination and DpnI digestion of the plasmid template in *Escherichia coli*. *Analytical Biochemistry*, *373*(2), 389–391.

Li, Y. (2012). Qinghaosu (artemisinin): Chemistry and pharmacology. *Acta Pharmacologica Sinica*, *33*(9), 1141–1146.

Liu, H., & Naismith, J. H. (2008). An efficient one-step site-directed deletion, insertion, single and multiple-site plasmid mutagenesis protocol. *BMC Biotechnology*, *8*(1), 91.

Liu, Z., Chen, O., Wall, J. B. J., Zheng, M., Zhou, Y., Wang, L., Ruth Vaseghi, H., Qian, L., & Liu, J. (2017). Systematic comparison of 2A peptides for cloning multi-genes in a polycistronic vector. *Scientific Reports*, *7*(1), 2193.

LU, F., HE, X.-L., Richard, C., & CAO, J. (2019). A brief history of artemisinin: Modes of action and mechanisms of resistance. *Chinese Journal of Natural Medicines*, *17*(5), 331–336.

Maier, A. G., & Rug, M. (2012). *In Vitro Culturing Plasmodium falciparum Erythrocytic Stages* (pp. 3–15).

Mao, Y. (2021). Structure, Dynamics and Function of the 26S Proteasome. In *Subcellular Biochemistry* (Vol. 96, pp. 1–151).

Marr, E. J., Milne, R. M., Anar, B., Girling, G., Schwach, F., Mooney, J. P., Nahrendorf, W., Spence, P. J., Cunningham, D., Baker, D. A., Langhorne, J., Rayner, J. C., Billker, O., Bushell, E. S., & Thompson, J. (2020). An enhanced toolkit for the generation of knockout and marker-free fluorescent *Plasmodium chabaudi*. *Wellcome Open Research*, *5*, 71.

Mbengue, A., Bhattacharjee, S., Pandharkar, T., Liu, H., Estiu, G., Stahelin, R. V., Rizk, S. S., Njimoh, D. L., Ryan, Y., Chotivanich, K., Nguon, C., Ghorbal, M., Lopez-Rubio, J.-J., Pfrender, M., Emrich, S., Mohandas, N., Dondorp, A. M., Wiest, O., & Haldar, K. (2015). A molecular mechanism of artemisinin resistance in *Plasmodium falciparum* malaria. *Nature*, *520*(7549), 683–687.

Milner, D. A. (2018). Malaria Pathogenesis. *Cold Spring Harbor Perspectives in Medicine*, *8*(1), a025569.

Mok, S., Ashley, E. A., Ferreira, P. E., Zhu, L., Lin, Z., Yeo, T., Chotivanich, K., Imwong, M., Pukrittayakamee, S., Dhorda, M., Nguon, C., Lim, P., Amaratunga, C., Suon, S., Hien, T. T., Htut, Y., Faiz, M. A., Onyamboko, M. A., Mayxay, M., … Bozdech, Z. (2015). Population transcriptomics of human malaria parasites reveals the mechanism of artemisinin resistance. *Science*, *347*(6220), 431–435.

Moxon, C. A., Gibbins, M. P., McGuinness, D., Milner, D. A., & Marti, M. (2020). New Insights into Malaria Pathogenesis. *Annual Review of Pathology: Mechanisms of Disease*, *15*(1), 315–343.

Mujtaba, T., & Dou, Q. P. (2011). Advances in the understanding of mechanisms and therapeutic use of bortezomib. *Discovery Medicine*, *12*(67), 471–480.

Ng, C. L., Fidock, D. A., & Bogyo, M. (2017). Protein Degradation Systems as Antimalarial Therapeutic Targets. *Trends in Parasitology*, *33*(9), 731–743.

Noedl, H., Se, Y., Schaecher, K., Smith, B. L., Socheat, D., & Fukuda, M. M. (2008). Evidence of Artemisinin-Resistant Malaria in Western Cambodia. *New England Journal of Medicine*.

Pannu, A. K. (2019). Malaria today: advances in management and control. *Tropical Doctor*.

Plewes, K., Leopold, S. J., Kingston, H. W. F., & Dondorp, A. M. (2019). Malaria. *Infectious Disease Clinics of North America*, *33*(1), 39–60.

Quadt, K. A., Smyrnakou, X., Frischknecht, F., Böse, G., & Ganter, M. (2020). *Plasmodium falciparum* parasites exit the infected erythrocyte after haemolysis with saponin and streptolysin O. *Parasitology Research*, *119*(12), 4297–4302.

Rashidi, S., Tuteja, R., Mansouri, R., Ali-Hassanzadeh, M., Shafiei, R., Ghani, E., Karimazar, M., Nguewa, P., & Manzano-Román, R. (2021). The main post-translational modifications and related regulatory pathways in the malaria parasite *Plasmodium falciparum*: An update. *Journal of Proteomics*, *245*, 104279.

Reilly, H. B., Wang, H., Steuter, J. A., Marx, A. M., & Ferdig, M. T. (2007). Quantitative dissection of clone-specific growth rates in cultured malaria parasites. *International Journal for Parasitology*, *37*(14), 1599–1607.

Rosenthal, M. R., & Ng, C. L. (2020). *Plasmodium falciparum* Artemisinin Resistance: The Effect of Heme, Protein Damage, and Parasite Cell Stress Response. *ACS Infectious Diseases*, *6*(7), 1599–1614.

Rosenthal, M. R., & Ng, C. L. (2021). A Proteasome Mutation Sensitizes P. falciparum Cam3.II K13 C580Y Parasites to DHA and OZ439. *ACS Infectious Diseases*, *7*(7), 1923–1931.

Rosenzweig, R., Bronner, V., Zhang, D., Fushman, D., & Glickman, M. H. (2012). Rpn1 and Rpn2 Coordinate Ubiquitin Processing Factors at Proteasome. *Journal of Biological Chemistry*, *287*(18), 14659–14671.

Ross, L. S., & Fidock, D. A. (2019). Elucidating Mechanisms of Drug-Resistant *Plasmodium falciparum*. *Cell Host & Microbe*, *26*(1), 35–47.

Sato, S. (2021). *Plasmodium*—a brief introduction to the parasites causing human malaria and their basic biology. *Journal of Physiological Anthropology*, *40*(1), 1.

Simon, C. S., Stürmer, V. S., & Guizetti, J. (2021). How Many Is Enough? - Challenges of Multinucleated Cell Division in Malaria Parasites. *Frontiers in Cellular and Infection Microbiology*, *11*.

Spence, P. J., Cunningham, D., Jarra, W., Lawton, J., Langhorne, J., & Thompson, J. (2011). Transformation of the rodent malaria parasite *Plasmodium chabaudi*. *Nature Protocols*, *6*(4), 553–561.

Stephens, R., Culleton, R. L., & Lamb, T. J. (2012). The contribution of *Plasmodium chabaudi* to our understanding of malaria. *Trends in Parasitology*, *28*(2), 73–82.

Stokes, B. H., Yoo, E., Murithi, J. M., Luth, M. R., Afanasyev, P., da Fonseca, P. C. A., Winzeler, E. A., Ng, C. L., Bogyo, M., & Fidock, D. A. (2019). Covalent *Plasmodium falciparum*-selective proteasome inhibitors exhibit a low propensity for generating resistance in vitro and synergize with multiple antimalarial agents. *PLOS Pathogens*, *15*(6), e1007722.

Sutherland, C. J., Henrici, R. C., & Artavanis-Tsakonas, K. (2020). Artemisinin susceptibility in the malaria parasite *Plasmodium falciparum*: propellers, adaptor proteins and the need for cellular healing. *FEMS Microbiology Reviews*.

Talman, A. M., Clain, J., Duval, R., Ménard, R., & Ariey, F. (2019). Artemisinin Bioactivity and Resistance in Malaria Parasites. *Trends in Parasitology*, *35*(12), 953–963.

Tilley, L., Straimer, J., Gnädig, N. F., Ralph, S. A., & Fidock, D. A. (2016). Artemisinin Action and Resistance in *Plasmodium falciparum*. *Trends in Parasitology*, *32*(9), 682–696.

Tse, E. G., Korsik, M., & Todd, M. H. (2019). The past, present and future of anti-malarial medicines. *Malaria Journal*, *18*(1), 93.

Tu, Y. (2016). Artemisinin-A Gift from Traditional Chinese Medicine to the World (Nobel Lecture). *Angewandte Chemie International Edition*, *55*(35), 10210–10226.

Vreden, S. G., Jitan, J. K., Bansie, R. D., & Adhin, M. R. (2013). Evidence of an increased incidence of day 3 parasitaemia in Suriname: an indicator of the emerging resistance of *Plasmodium falciparum* to artemether. *Memórias Do Instituto Oswaldo Cruz*, *108*(8), 968–973.

Wang, L., Delahunty, C., Fritz-Wolf, K., Rahlfs, S., Helena Prieto, J., Yates, J. R., & Becker, K. (2015). Characterization of the 26S proteasome network in *Plasmodium falciparum*. *Scientific Reports*, *5*(1), 17818.

Weiss, D. J., Lucas, T. C. D., Nguyen, M., Nandi, A. K., Bisanzio, D., Battle, K. E., Cameron, E., Twohig, K. A., Pfeffer, D. A., Rozier, J. A., Gibson, H. S., Rao, P. C., Casey, D., Bertozzi-Villa, A., Collins, E. L., Dalrymple, U., Gray, N., Harris, J. R., Howes, R. E., … Gething, P. W. (2019). Mapping the global prevalence, incidence, and mortality of *Plasmodium falciparum*, 2000–17: a spatial and temporal modelling study. *The Lancet*, *394*(10195), 322–331.

White, N. J. (2017). Malaria parasite clearance. *Malaria Journal*, *16*(1), 88.

Wicht, K. J., Mok, S., & Fidock, D. A. (2020). Molecular Mechanisms of Drug Resistance in *Plasmodium falciparum* Malaria. *Annual Review of Microbiology*, *74*(1), 431–454.

Witkowski, B., Khim, N., Chim, P., Kim, S., Ke, S., Kloeung, N., Chy, S., Duong, S., Leang, R., Ringwald, P., Dondorp, A. M., Tripura, R., Benoit-Vical, F., Berry, A., Gorgette, O., Ariey, F., Barale, J.-C., Mercereau-Puijalon, O., & Menard, D. (2013). Reduced Artemisinin Susceptibility of *Plasmodium falciparum* Ring Stages in Western Cambodia. *Antimicrobial Agents and Chemotherapy*, *57*(2), 914–923.

World Health Organization. (2020). World Malaria Report 2020. In *World Health: Vol. WHO/HTM/GM* (Issue November).

Xie, S. C., Ralph, S. A., & Tilley, L. (2020). K13, the Cytostome, and Artemisinin Resistance. *Trends in Parasitology*, *36*(6), 533–544.

Yam, X. Y., & Preiser, P. R. (2017). Host immune evasion strategies of malaria blood stage parasite. *Molecular BioSystems*, *13*(12), 2498–2508.

Yang, P.-C., & Mahmood, T. (2012). Western blot: Technique, theory, and trouble shooting. *North American Journal of Medical Sciences*, *4*(9), 429.

Yang, T., Yeoh, L. M., Tutor, M. V., Dixon, M. W., McMillan, P. J., Xie, S. C., Bridgford, J. L., Gillett, D. L., Duffy, M. F., Ralph, S. A., McConville, M. J., Tilley, L., & Cobbold, S. A. (2019). Decreased K13 Abundance Reduces Hemoglobin Catabolism and Proteotoxic Stress, Underpinning Artemisinin Resistance. *Cell Reports*, *29*(9), 2917-2928.e5.

Zekar, L., & Sharman, T. (2020). *Plasmodium falciparum* Malaria. In *STAT Pearls*.

Zerfas, B. L., Coleman, R. A., Salazar-Chaparro, A. F., Macatangay, N. J., & Trader, D. J. (2020). Fluorescent Probes with Unnatural Amino Acids to Monitor Proteasome Activity in Real-Time. *ACS Chemical Biology*, *15*(9), 2588–2596.

Zhang, J., Feng, G.-H., Zou, C.-Y., Su, P.-C., Liu, H.-E., & Yang, Z.-Q. (2017). Overview of the improvement of the ring-stage survival assay – a novel phenotypic assay for the detection of artemisinin-resistant *Plasmodium falciparum*. *Zoological Research*, *38*(6), 317–320.

Zhang, M., Gallego-Delgado, J., Fernandez-Arias, C., Waters, N. C., Rodriguez, A., Tsuji, M., Wek, R. C., Nussenzweig, V., & Sullivan, W. J. (2017). Inhibiting the *Plasmodium* eIF2α Kinase PK4 Prevents Artemisinin-Induced Latency. *Cell Host & Microbe*, *22*(6), 766-776.e4.

# Supplementary Information

## Annex A: Protein Sequence Alignment

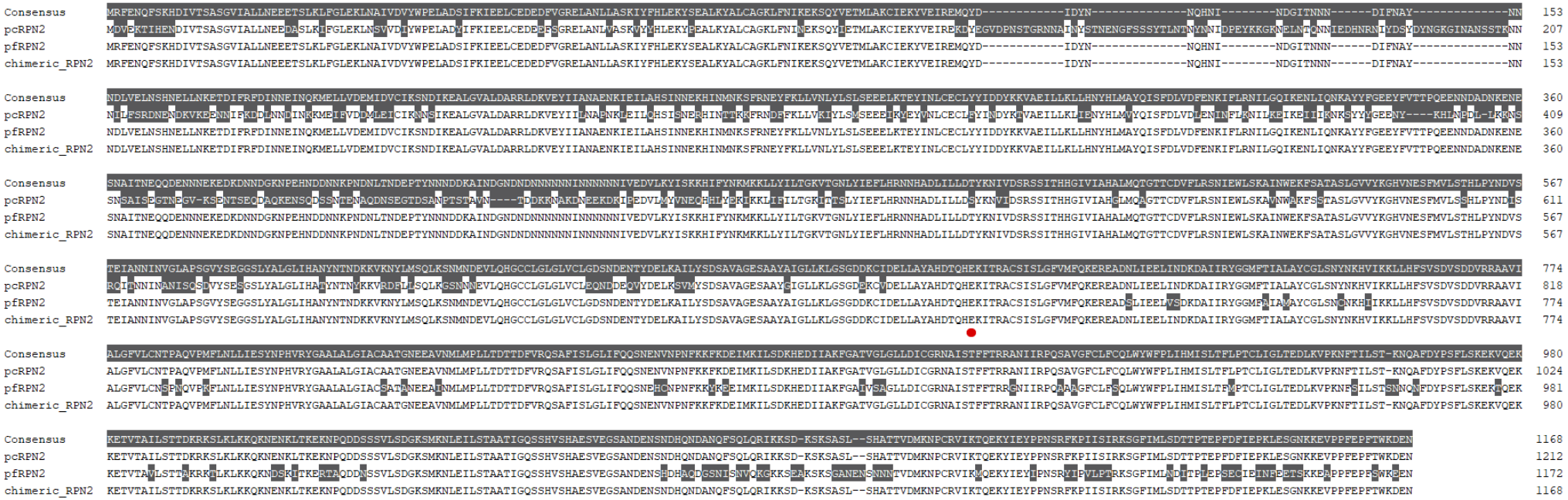

## Annex B: Bovine Serum Albumin (BSA) curve

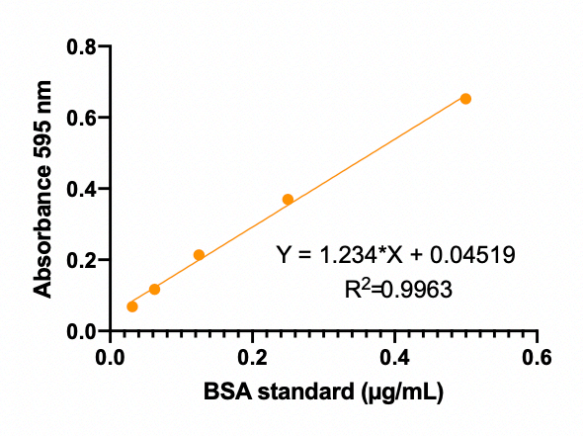


**Figure A1. BSA standard curve.** In a standard reaction, 10 µL of each BSA concentration was mixed with 200 µL of Bradford reagent and allowed to stand at RT for 5 min. Each sample was measured for absorbance at 595 nm against a blank.